

A Practical Algorithm with Performance Guarantees for the Art Gallery Problem

Simon Hengeveld¹ and Tillmann Miltzow^{*1}

¹Department of Computer Science, Utrecht University, t.miltzow@googlemail.com
s.b.hengeveld@students.uu.nl

Abstract

Given a closed simple polygon P , we say two points p, q see each other if the segment $\text{seg}(p, q)$ is fully contained in P . The art gallery problem seeks a minimum size set $G \subset P$ of guards that sees P completely. The only currently correct algorithm to solve the art gallery problem exactly uses algebraic methods and is attributed to Sharir [21]. As the art gallery problem is $\exists\mathbb{R}$ -complete [3], it seems unlikely to avoid algebraic methods, for any exact algorithm, without additional assumptions.

In this paper, we introduce the notion of *vision-stability*. In order to describe vision-stability consider an *enhanced* guard that can see “around the corner” by an angle of δ or a *diminished* guard whose vision is by an angle of δ “blocked” by reflex vertices. A polygon P has vision-stability δ if the optimal number of enhanced guards to guard P is the same as the optimal number of diminished guards to guard P . We will argue that most relevant polygons are vision-stable. We describe a *one-shot vision-stable* algorithm that computes an optimal guard set for vision-stable polygons using polynomial time and solving one integer program. It guarantees to find the optimal solution for every vision-stable polygon. We implemented an *iterative vision-stable* algorithm and show its practical performance is slower, but comparable with other state of the art algorithms. Our iterative algorithm is inspired and follows closely the one-shot algorithm. It delays several steps and only computes them, when deemed necessary.

Given a chord c of a polygon, we denote by $n(c)$ the number of vertices visible from c . The *chord-visibility width* ($\text{cw}(P)$) of a polygon is the maximum $n(c)$ over all possible chords c . The set of vision-stable polygons admit an FPT algorithm, when parametrized by the chord-visibility width. Furthermore, the one-shot algorithm runs in FPT time, when parametrized by the number of reflex vertices. These are the first two FPT algorithms for the art gallery problem.

^{*}The second author is supported by the NWO Veni grant EAGER.

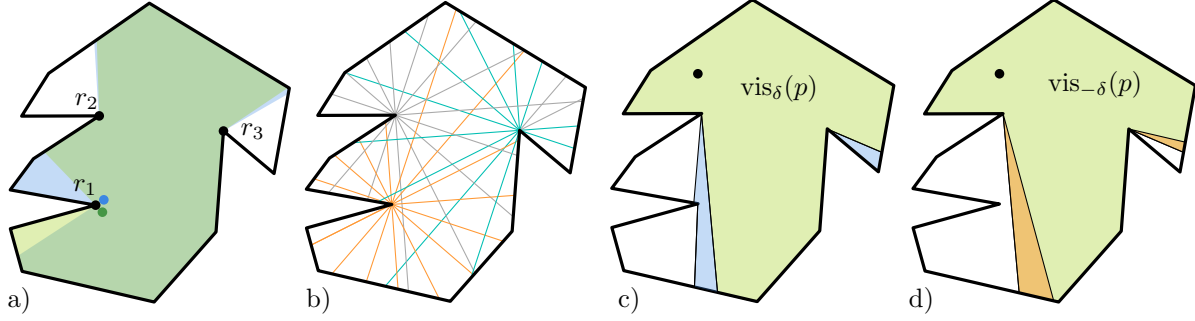


Figure 1: a) The small change in position changes a lot by how much the reflex vertex r_1 blocks the respective visibility of the two guards, but it only has a small effect on the way that r_2 or r_3 blocks the visibility of the guards. b) Shooting rays from reflex vertices. c) Enhanced visibility region. d) Diminished visibility region.

1 Introduction

For most algorithmic problems, there is a *practice-theory gap*. That is a gap between algorithms that perform best in practice and that perform best in theory. In this work, we narrow this gap for the art gallery problem. We present an algorithm that has *both* theoretical performance guarantees and performs well in practice.

On the theory side, we know that the art gallery problem is decidable using tools from real algebraic geometry. The idea is to encode guards by real numbers and use polynomial equations and inequalities to encode visibility [21]. Currently, researchers working on solving polynomial equations repeatedly report that 12 is the maximum number of variables they could handle, using exact methods. (The second author asked this at several conferences and workshops.) To express the art gallery problem by polynomial equations has a considerable blow up and needs existentially and universally quantified variables. In summary, we would be surprised, if these exact methods could even find an optimal solution of size two for the art gallery problem. As the art gallery problem is $\exists\mathbb{R}$ -complete [3], we know that methods from real algebraic geometry are unavoidable for any exact algorithm, without additional assumptions.

On the practical side, various researchers implemented algorithms and found the optimal solution on synthetic instances of up to 5000 vertices [7, 13, 14, 17–19, 23, 28, 31]. The idea is to discretize the problem and hope that the solution to the discretized problem also gives the optimal solution to the original problem. To be more specific, the approach is to generate a *candidate* set C and a *witness* set W . Then compute the optimal way to guard W using the minimum number of guards in C . In an iterative manner, more candidates and witnesses are generated until the optimal solution is found. While those algorithms *usually* find the optimal solution, there is a simple polygon on which those algorithms run *forever* [2]. We do not know sufficient conditions under which those algorithms would give the optimal solution in a finite amount of time. Let us emphasize that without additional assumptions it is not possible to prove any run time guarantees on those algorithms, unless $\text{NP} = \exists\mathbb{R}$.

In this paper, we introduce the notion of vision-stability. We argue that most practical polygons are vision-stable. Using this assumption, we develop the *one-shot (vision-stable)* algorithm that is *guaranteed* to find an optimal solution for every vision-stable polygon. The algorithm takes

polynomial time and solves one integer program. In particular, this shows that the art gallery problem is in NP for vision-stable polygons. We refine the algorithm and present the *iterative (vision-stable)* algorithm. The iterative algorithm is also guaranteed to find the optimal solution for every vision-stable polygon. It runs in polynomial time and solves at most a polynomial number of integer programs. Both algorithms are *reliable*, in the sense that even if the input polygon is not vision-stable, the reported result is correct. We implemented and tested the iterative algorithm. Our test results are slower, but comparable with previous practical algorithms. Thus the iterative vision-stable algorithm is practical and has theoretical performance guarantees.

Before we formally define the notion of vision-stability, which is the key concept of this paper, let us give some basic intuition on discretizing the art gallery problem. The aim of the discretization process is to define a suitable *candidate set* C such that $\text{opt}[C]$, the optimum guard set restricted to C , is “pretty close” to the actual optimum opt . After defining C in a suitable fashion, we can compute $\text{opt}[C]$ by solving an integer program. We know [11] that the grid $\Gamma = w\mathbb{Z}^2 \cap P$ with a small enough width w is a good such candidate set in the sense that $|\text{opt}[\Gamma]| \leq 10|\text{opt}|$, under some mild general position assumptions. Using smoothed analysis [20, 22] and a suitable random model of perturbation, we even know that $|\text{opt}[\Gamma]| = |\text{opt}|$, with high probability. In summary, a fine enough grid contains the optimal solution, under certain assumptions, however the size of the candidate set C is also important. The grid Γ as described above has exponential size in terms of the input. Thus computing $\text{opt}[\Gamma]$ is infeasible in practice, making it very desirable to attain a candidate set C with similar properties as Γ and of polynomial size.

As a first step, we realize that a *uniformly distributed* candidate set would either be too large or too coarse. Thus at some spots, we want the candidate set to be more dense and at other places in the polygon we want it to be more sparse. Let us say two guard positions g, g' have almost the same visibility region then hopefully it is not so important to keep track of both positions, but keeping only one of the positions is hopefully sufficient. Thus if the visibility regions of g and g' are very different, we should potentially include both of them in our candidate set C . Another, almost trivial, observation is that a small movement of g towards g' may dramatically change visibility regions, if g and g' are close to a reflex vertex. If g and g' are both very far away from all reflex vertices their visibility regions change almost not at all, see Figure 1 a).

This motivates the following approach. Shoot rays from every reflex vertex, such that the angle between any two rays is at most some given angle δ . This defines an arrangement \mathcal{A} . All intersection points of the rays within the polygon P define our candidate set C , see Figure 1 b). On an intuitive level, for every point $p \in P$ there is a candidate $c \in C$ such that the visibility regions of p and c are similar. When r denotes the number of reflex vertices, we get a total number of rays upper bounded by $O(\frac{r}{\delta})$. It follows that the candidate set has size $O(\frac{r^2}{\delta^2})$. The definition of vision-stability is fairly technical and we refer the reader to Section 2. The intuition is as follows. We will define a notion of enhanced and diminished visibility regions of points, denoted by $\text{vis}_\delta(p)$ and $\text{vis}_{-\delta}(p)$, as depicted on the right of Figure 1. We say a set G is δ -guarding, if $\bigcup_{g \in G} \text{vis}_\delta(g) = P$. We denote by $\text{opt}(P, \delta)$ the size of the minimum δ -guarding set. We say a polygon has vision-stability δ if $\text{opt}(P, -\delta) = \text{opt}(P, \delta)$. Note that for $\delta' > \delta > 0$, it holds that P has vision-stability δ' implies that P also has vision-stability δ . See Section 2.2, for an in depth justification about vision-stability. Here, we give only a very brief summary. First, without any assumption, we cannot avoid algebraic methods unless $\text{NP} = \exists\mathbb{R}$. Second, there are arguments related to smoothed analysis, which suggest that most polygons are vision-stable, when considering appropriate probability spaces. Third, our algorithms were able to solve *all* instances, that we

tried. Note that we cannot compute if a polygon has vision-stability δ . Therefore, it is important that our algorithms work correctly even if the underlying polygon is not vision-stable. Specifically, our algorithms will either compute the optimal solution or report that the input polygon had lower vision-stability than specified by the user. We say our algorithms are *reliable*, as they never return an incorrect answer. Using vision-stability, we exhibit a candidate set C of polynomial size. The idea is to use the vertices of arrangement \mathcal{A} from Figure 1 b). For technical reasons, we will not use the arrangement \mathcal{A} itself, but a refinement of it, as explained in Section 3. Note that the smaller the vision-stability, the weaker the assumption on the underlying polygon and thus the larger the candidate set needs to be.

Theorem 1 (Candidate Set). *Given a polygon with vision-stability δ and r reflex vertices, it is possible to compute a candidate set C (of size $O(\frac{r^4}{\delta^2})$) in polynomial time on a real RAM. The candidate set C contains an optimal solution.*

Let us give an intuition of the proof idea of Theorem 1. As mentioned before, we use all the vertices of a refinement of the arrangement \mathcal{A} , as in Figure 1, as our candidate set C . Consider a minimum size set G_0 that is $(-\delta)$ -guarding P . Replace each guard $g \in G_0$ by a guard $g' \in C$ that is “close by”. This gives a new solution $G_1 \subseteq C$ of equal size. Using that G_0 is $(-\delta)$ -guarding, we can show that G_1 is guarding P in the usual sense. As $\text{opt}(P, -\delta) = \text{opt}(P, 0) = \text{opt}(P, \delta)$, we can conclude that $G_1 \subseteq C$ is of minimum size.

Theorem 1 answers an open question by de Rezende et al. [19], for vision-stable polygons. “Therefore, it remains an important open question whether there exists a discretization scheme that guarantees that the algorithm always converges [...]” This easily leads to an algorithm that avoids algebraic methods. The idea is to use faces and vertices of some arrangement as candidates and witnesses. We build an integer program to find the minimum number of guards. We will show that the algorithm will report only point guards, if the underlying polygon is vision-stable.

Theorem 2 (One-Shot vision-stable Algorithm). *Let P be an n vertex polygon, with vision-stability δ and r reflex vertices. We assume that δ is given as part of the input. Then the one-shot algorithm has a preprocessing time of $O(\frac{r^8}{\delta^4} \log n)$ on a real RAM and additionally solves exactly one integer program. The algorithm either returns the optimal solution or it reports that the vision-stability is smaller than δ .*

As the size of the integer program only depends on r and $1/\delta$, it exhibits an FPT algorithm, with respect to the number of reflex vertices r , for every fixed δ . The most natural parameter for the art gallery problem is the solution size. As the art gallery problem is W[1]-hard, when parameterized by the solution size [12], research focused on other parameters [4–6, 8, 26, 27]. Specifically, Agrawal et al. [4] described an elegant FPT algorithm for the art gallery problem. They considered three variants of the art gallery problem defined by restricting guard positions and the part of the polygon that needs to be guarded. By considering the number of reflex vertices as the parameter, they answered a question by Giannopoulos, for those variants. “Guarding simple polygons has been recently shown to be W[1]-hard w.r.t. the number of (vertex or point) guards. Is the problem FPT w.r.t. the number of reflex vertices of the polygon?” [24]. We answer the same question, with respect to vision-stable polygons and the classic variant of the art gallery problem.

Corollary 3 (Reflex-FPT Algorithm). *Given a vision-stable polygon, with any fixed vision-stability. The one-shot algorithm is FPT with respect to the number of reflex vertices.*

Although the one-shot algorithm does not require algebraic methods and only polynomial pre-processing time, it is still way too slow to be considered practical. Note that the performance bottleneck is not solving the integer program, but computing visibilities. As a next step, we develop the *iterative vision-stable* algorithm, see Section 4. It is more practical and retains similar theoretical performance guarantees. Note that the statement that an algorithm is both practical and theoretical must be taken with caution. Once we have a *practical* algorithm \mathcal{P} and a *theoretical* algorithm \mathcal{T} , we can easily get a third algorithm \mathcal{B} that has *both* properties as follows. Run algorithm \mathcal{P} within the running time bound of \mathcal{T} . If \mathcal{P} does not return a solution abort and run \mathcal{T} . Here, \mathcal{T} serves as a *safe guard* for \mathcal{P} . Clearly \mathcal{B} performs as well in practice as \mathcal{P} and has the theoretical bounds of \mathcal{T} . Thus, when we say that we show theoretical performance guarantees of some algorithm, we should really ask ourselves, if we show those guarantees for the algorithm that we actually use or for some safe guards that aren't ever used in practice.

The core idea of the iterative algorithm is as follows. We start with a very coarse arrangement \mathcal{A} . Using the faces and the vertices of \mathcal{A} , we define a candidate set C and a witness set W . We compute which candidates see which witnesses. This enables us to build an integer program, that tries to find a minimum guard set $G \subseteq C$, that sees all the vertex-witnesses. Note that vertices and faces may serve as guards and some face-witnesses may be unguarded. As a secondary objective function the integer program tries to minimize the number of face-guards used in G and the number of unseen face-witnesses. If the guard set G contains only point guards and sees all face-witnesses, the iterative algorithm reports the optimal solution. Otherwise, it refines the arrangement \mathcal{A} and goes to the next iteration. The iterative algorithm performs reasonably well in practice and we can show the following theorem.

Theorem 4 (Iterative Algorithm). *Let P be an n vertex polygon, with vision-stability δ . Then the iterative algorithm returns the optimal solution to the art gallery problem. It has a running time of $(\frac{n}{\delta})^{O(1)} + T$ per iteration and takes at most $(\frac{n}{\delta})^{O(1)}$ iterations. Here T denotes the time it takes to solve one integer program.*

Although Theorem 4 is weaker than Theorem 2 from a theoretical perspective, we find it more interesting as the iterative algorithm can be considered practical. This also makes the proof more involved.

We use heuristics to bring down the number of visibilities between candidates and witnesses that we have to compute. One of them is to benefit from low local complexity of the input polygons. Interestingly, this inspired a new structural parameter, which we call the chord-visibility width. Given a chord c of P , we denote by $n(c)$ the number of vertices visible from c . The *chord-visibility width* ($\text{cw}(P)$) of a polygon is the maximum $n(c)$ over all possible chords c . We think that the chord-visibility width is an interesting parameter in its own right. We show that the art gallery problem is FPT with respect to the chord-visibility width, see Section 5.

Theorem 5 (Chord-Width-FPT). *Let P be a simple vision-stable polygon. Then there is an FPT algorithm for the art gallery problem with respect to the chord-visibility width.*

The core idea is to decompose the polygon into weak visibility polygons of low complexity, see Section 4.1 and Figure 8. Those weak visibility polygons define the *weak visibility polygon tree* T . As visibilities of witnesses and candidates only interact between child-parent nodes and siblings in T , we design a simple bottom-up dynamic program on the nodes of T .

As mentioned earlier, we implemented and tested the iterative algorithm on input polygons of several sizes, see Section 6. Specifically, 30 instances of polygons of sizes 60, 100, 200 and 500

vertices. These tests demonstrate that the running time of the algorithm in practice is not far behind the times found by Tozoni et al. [31]. Another interesting finding is that the running time of the algorithm appears to correlate with the measured vision-stability of the input polygons, within each size group. The running time is dominated by visibility queries and solving integer programs was only a small part of the CPU work load. Finally, we show that the implementation of the algorithm provides a rapidly improving solution even for polygons that are not vision-stable. Specifically, Abrahamsen et al. [2] introduced a small and simple polygon, which requires irrational guards for an optimal guarding. Although, the iterative algorithm avoids irrational numbers it returns a solution G_i after the i^{th} iteration. It seems that G_i converges quickly to (but never reaches) the optimum.

Future Research. The vast majority of the work on the art gallery problem focused on variants of the classic question. There are almost no positive theoretical algorithmic results on the original art gallery problem, with some exceptions [9, 11, 21]. We believe that the main reason for this focus on variants is the fact that the art gallery problem is inherently continuous, as is reflected by the $\exists\mathbb{R}$ -completeness [3]. In other words, no discretization of the solution space was known. Now that we arguably broke that barrier, we hope that more progress will be made on the original problem.

Let us name a few concrete directions for future work. A practical shortcoming of our algorithms compared to previous algorithms are very slow segment-vertex visibility queries. One intriguing open question is to make those faster. Can we carry over the results of this paper to polygonal domains with holes? Does the iterative algorithm always converge towards the optimal solution, even if the underlying polygon is not vision-stable? Can we remove some of the safe guards and still show correctness of the iterative algorithm? Can we show correctness of other algorithms using vision-stability? All the presented bounds are very large. So a natural question is to lower them. For instance, is there a single exponential FPT algorithm with respect to the reflex vertices or the chord-visibility width? What is the smallest candidate set that we can compute in polynomial time?

2 Vision Stability

In this section, we define the notion of *vision-stability*, and give a justification, why we believe that typical polygons are vision-stable in practice. At last, we will show some important properties, which are related to vision-stability.

2.1 Definition

In a nutshell, enhanced and diminished vision are artificial ways of vision, where we can either “look around a corner” or are “more blocked” by a corner than we would expect. The notion vision-stability entails that either enhancing or diminishing the vision does not change the optimal number of guards.

Given a simple polygon P and a point q , the visibility region of q is defined as $\text{vis}(q) = \{x \in P : x \text{ sees } q\}$. Let r be a reflex vertex of P and we assume that q sees r . Then, given some $\delta > 0$, we can define the *visibility enhancing region* $A = A(q, r, \delta)$ as follows. Rotate a ray v with apex r by some angle of δ , clockwise and counter-clockwise. At each time of the rotation the ray v defines a maximal segment inside P with endpoint r . In some cases, the segment is the single point r , see Figure 2 c). The region $A(r, \delta)$ is the union of all those segments. See the blue region in Figure 2 c).

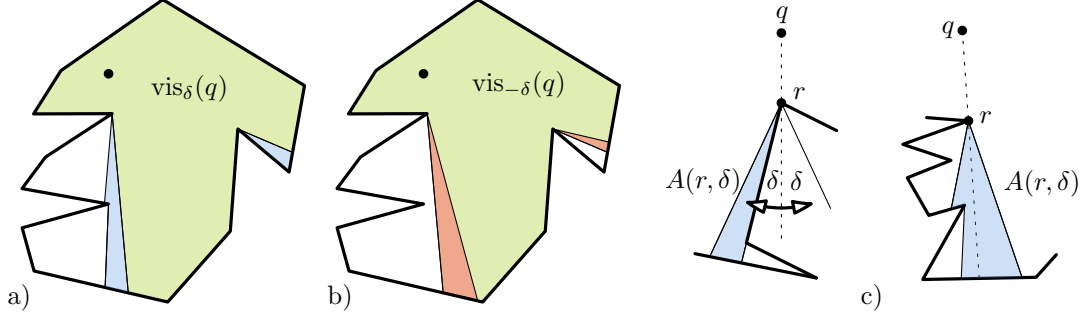


Figure 2: a) The visibility of the point q in green. The blue region enhanced the visibility. b) The red region diminishes the visibility of q . c) A ray is rotated around a reflex vertex r . It defines a region that is either added or removed from the visibility region.

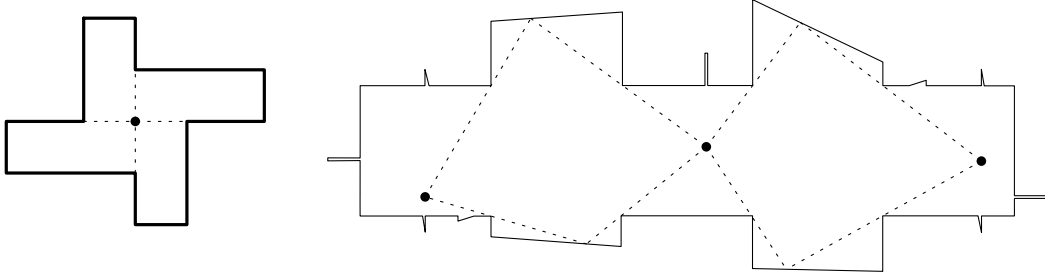


Figure 3: Left: The polygon has a unique guarding that relies on simple collinearities. Right: This polygon has a unique irrational guarding with three guards [2].

For some $\delta > 0$, we define the δ -enhanced visibility region $\text{vis}_\delta(q)$ of q as $\text{vis}(q)$ and for every suitable reflex vertex, we add the region $A(r, \delta)$. We define the δ -diminished visibility region $\text{vis}_{-\delta}(q)$ of q as $\text{vis}(q)$ after we remove the regions $A(r, \delta)$, for every applicable reflex vertex r . To be precise, we define $\text{vis}_\delta(q)$ to be a closed set, both for $\delta > 0$ and $\delta \leq 0$.

Given a polygon P , we say that G is δ -guarding P if $\bigcup_{g \in G} \text{vis}_\delta(g) = P$. We denote by $\text{opt}(P, \delta)$ the size of the minimum δ -guarding set. For brevity, we denote $\text{opt}(P, 0)$, merely by $\text{opt}(P)$ or, if P is clear from the context, by opt . We say that a polygon P is *vision-stable* or equivalently has vision-stability $\delta > 0$, if $\text{opt}(P, -\delta) = \text{opt}(P, \delta)$.

2.2 Justification

In this section, we try to reflect on different aspects of the definition of vision-stability.

Consider polygon P_1 , to the left of Figure 3. It is not vision-stable. That this simple example is not vision-stable is clearly a weakness of the concept. Note that this example relies on collinearities. Many computational geometry papers assume general position of the the underlying point set. Those assumptions are made for two reasons. The first is that collinearities are very unlikely, if we think about some random model that generates our point set. The second reason is that collinearities can often be handled in practice, and the details are left out as they are very tedious, but add little to nothing to the underlying algorithmic concepts. Our algorithms are also able to find the optimum for these types of situations in practice.

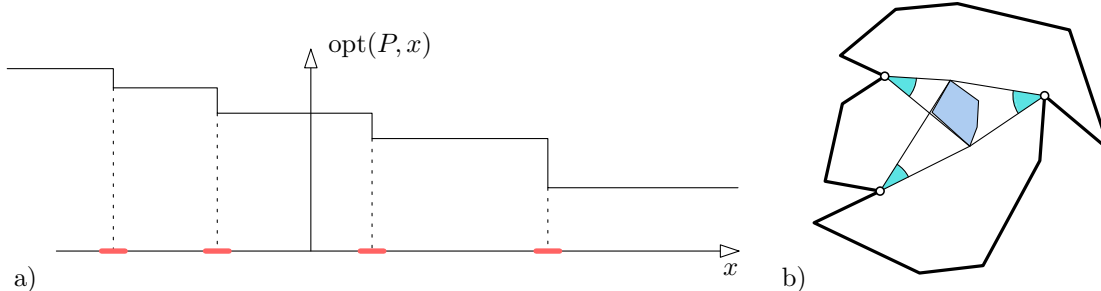


Figure 4: a) There are at most n intervals of length 2δ each. b) Illustration of the power of a face.

Let us now give another example of a polygon P_2 that is not vision-stable, see to the right of Figure 3. The polygon P_2 has a unique guarding with irrational guards. Although it has plenty of collinearities, it can be modified not to have those collinearities. Polygons similar to P_2 exist and the irrational coordinates required for an optimal guarding might need arbitrarily large algebraic degree [3]. We see the existence of such polygons as a strong argument for the need of additional assumptions. In particular, those polygons show that *without* additional assumptions algebraic methods are unavoidable. Furthermore, they show that the art gallery problem is $\exists\mathbb{R}$ -complete [3].

As a third aspect for vision-stability, we want to argue that polygons similar to P_2 are very rare in practice. Note that polygon P_2 was only found after four decades of research on the art gallery problem. It took the right approach, computer assistance and tedious trial and error to find this polygon. Thus it is no surprise that as of this writing no second similar polygon is known yet. There are polygons that are slight modifications of P_2 and the polygons that stem from the $\exists\mathbb{R}$ -hardness proofs are the only exceptions [3].

There is a fourth consideration. We will present an algorithm based on vision-stability in Section 4. As we will see in our test results in Section 6, the algorithm gives a sequence $(G_i)_{i \in \mathbb{N}}$ of guarding sets. We observe that this sequence empirically approaches the actual optimal guarding for P_2 , see Figure 14. In other words, it could be that the algorithm described hence forth has the property that it always converges to the optimal solution, even if the underlying polygon is not vision-stable. It is a tantalizing open question, if this always happens or whether it is just a lucky coincidence that happened with P_2 . Unfortunately, we don't know another polygon that we could potentially use to test this conjecture empirically.

A fifth argument can be made that resembles ideas from smoothed analysis. Fix some polygon P for the following discussion. Consider a world, where people would actually care for computing $\text{opt}(P, x)$, for values of x other than zero. We define the event that $\text{opt}(P, x - \delta) = \text{opt}(P, x + \delta)$ by $E(x, \delta)$. In this case, we say that P is x -vision-stable, with vision-stability δ . In other words, the event $E(x, \delta)$ represents vision-stability for the task of computing $\text{opt}(P, x)$, instead of $\text{opt}(P, 0)$. In particular $E(0, \delta)$ corresponds to P being vision-stable in the usual sense. We show the following lemma.

Lemma 6. *Let P be any simple polygon on n vertices. Choose $x \in [-1/2, 1/2]$ uniformly at random. Then it holds that $\Pr(E(x, \delta)) \geq 1 - 2\delta n$.*

This lemma says that any simple polygon P is x -vision-stability with high probability. We want to argue that as $E(x, \delta)$ has high probability, then on an *intuitive level*, the same should be true for $E(\delta)$. The reason being that $E(x, \delta)$ and $E(P, 0)$ may be regarded as mathematically

equally valuable. Let us point out that this is purely an intuition that may not be shared by everyone. In particular, as P is fixed, the event $E(0, \delta)$ either happens or doesn't happen. There is no mathematically defined probability space that we could talk about. Also note that $\text{opt}(P, x)$, for $x \neq 0$, has, to the best of our knowledge, never been studied before.

Proof of Lemma 6. We consider the function

$$f : [-1/2, 1/2] \rightarrow \mathbb{N}, \quad x \mapsto \text{opt}(P, x).$$

See Figure 4 a) for an illustration of f . The function f is monotone as visibility regions only get larger with larger x , thus it becomes easier to guard. Clearly, we need at least one guard and most n guards, if n is the number of vertices of P . Thus f has at most $n-1$ breakpoints. Given some x , the event $E(x, \delta)$ is equivalent to the fact that there is no breakpoint within distance δ of x . Taking the union of all the intervals of length 2δ centered at the breakpoints yields $\Pr(E(x, \delta)) \geq 1 - 2\delta n$. \square

Let us mention a sixth aspect of vision-stability. Our practical algorithm computes on the fly an upper bound on the vision-stability of the underlying polygon. This upper bound has a large explanatory value in understanding practical running times, as we will explain further in Section 6.1. Interestingly the running time of equally sized polygons vary easily within a factor of 10. In many cases, it seems to be the case that polygons with a high running time have a low vision-stability, see Section 6.1.

In summary additional assumptions should always be treated with some amount of caution. We consider different aspects in favor of the usage of our new assumption. We are looking forward to a lively discussion in the research community.

2.3 Power of a Face.

One of the key concepts of our algorithms is the power of a face. Assume, we are given a point g contained in a convex set f . Clearly, f sees at least as much as g . If g and f see the same set of reflex vertices then we can think of f as “seeing around the corner” a little bit more than g . The power of f is a simple to calculate approximation of the degree to which f “sees around the corner”.

For the following description consider Figure 4 b). For each reflex vertex r , we define the power-angle $\alpha(r)$, as the angle of the minimum cone with apex r that fully contains f . The *power* of the face f as the maximum of all the $\alpha(r)$, for r visible from f , i.e., $\text{power}(f) = \max_{r \in \text{vis}(f)} \alpha(r)$.

We denote by $\text{chord}(a, b)$ the chord in P that contains the two distinct points a, b , if it exists. The set $\text{chord}(A, B) = \{\text{chord}(a, b) : a \in A, b \in B, a \neq b, a \text{ sees } b\}$. Let R denote the set of reflex vertices of P . We refer to a chord $c \in \text{chord}(R, R)$ as a *reflex chord*. Reflex chords play a major role in proving correctness of our algorithms. One of its first appearances can be seen in the following lemma.

Lemma 7. *Let P be a simple polygon and let f be a face that is not properly intersected by any reflex chord. Furthermore let r be a reflex vertex that sees at least one interior point of f . Then it holds that r sees the entire face f .*

Proof. As $\text{vis}(r)$ is a closed region, we know that r sees f if and only if it sees all its interior points. For the purpose of contradiction assume that there is an interior point that is not seen by r . Consider the boundary b of $\text{vis}(r) \cap f$. This segment b is part of a reflex chord, which properly intersects f . This is a contradiction to the assumption. \square

Given a convex polygon f in some polygon P , we denote by $\text{representative}(f)$ a point of f to represent the face. In case that f has a reflex vertex r , we set $\text{representative}(f) = r$. Otherwise, we choose the lexicographically smallest vertex in f that is not a convex vertex of P . (In principle, we could choose any point in f arbitrarily. We exclude convex vertices of P , as this will allow us to describe an FPT algorithm later most conveniently. For concreteness, we pick the lexicographically smallest.) If we are given a set F of faces then we define $\text{representative}(F) = \{\text{representative}(f) : f \in F\}$. Given a set f in the plane, we denote by $\text{int}(f)$ the interior points of f .

In a simplified way the following lemma states that the visibility of a face f can be replaced by the visibility of a single point $p \in f$ with enhanced vision. This point p is called the representative as defined above. We want to point out that if a face contains a reflex vertex r , then this reflex vertex may see much more than the remainder of the face. Therefore, we defined the representative to be this reflex vertex in the applicable cases. Even more the enhanced representative can even see a complete face f' that was only partially visible from f . Again, there is a degenerate case that we have to exclude. To be precise, if f only sees a reflex vertex then enhancing the visibility by δ may not be helpful. See Figure 5, for an illustration of both special cases.

Lemma 8 (Face-Point-Replacement). *Assume the following conditions are met.*

- *We are given a simple polygon P .*
- *Two closed convex regions f, f' with $\text{power}(f), \text{power}(f') \leq \delta/2$ are given.*
- *Neither f nor f' are properly intersected by a reflex chord.*
- *The region f has at most one reflex vertex of P on its boundary.*
- *$\text{vis}_\gamma(f) \cap \text{int}(f') \neq \emptyset$, for some $\gamma \in [-\delta, 0]$.*
- *We denote $p = \text{representative}(f)$.*

Then it holds that $f' \subseteq \text{vis}_{\gamma+\delta}(p)$.

Admittedly, the lemma is already technical. Before we prove the lemma let us point out a simple corollary, which is slightly less technical. Unfortunately, Corollary 9 will not be strong enough for our purposes.

Corollary 9. *Let P be a simple polygon. Assume the following conditions are met.*

- *A convex region $f \subseteq P$ with $\text{power}(f) \leq \delta/2$ is given and no reflex chord properly intersects f .*
- *The region f has at most one reflex vertex of P on its boundary.*
- *We denote $p = \text{representative}(f)$.*
- *A number $\gamma \in [-\delta, 0]$ is given.*

Then it holds that $\text{vis}_\gamma(f) \subseteq \text{vis}_{\gamma+\delta}(p)$.

Proof Corollary 9. It is easy to construct an arrangement \mathcal{A} such that every face in \mathcal{A} has small power and is not split by a reflex chord. Let f' be a face of \mathcal{A} . If $\text{vis}_\gamma(f)$ contains an interior point of f' , then by Lemma 8 it holds that $f' \subseteq \text{vis}_{\gamma+\delta}(p)$. This finishes the proof. \square

Proof Lemma 8. Let $q \in \text{int}(f')$ be an arbitrary interior point of f' . We will show that $q \in \text{vis}_{\gamma+\delta}(p)$. This is sufficient as visibility regions are closed by definition and thus $\text{vis}_{\gamma+\delta}(p) \supseteq \text{int}(f') \Rightarrow \text{vis}_{\gamma+\delta}(p) \supseteq f'$.

Let $a \in f$ be a point that sees some other point $b \in \text{int}(f')$. Such a pair (a, b) exists by the assumption $\text{vis}_\gamma(f) \cap \text{int}(f') \neq \emptyset$ and the fact that $\text{vis}_\gamma(f) \subseteq \text{vis}(f)$, for $\gamma \leq 0$.

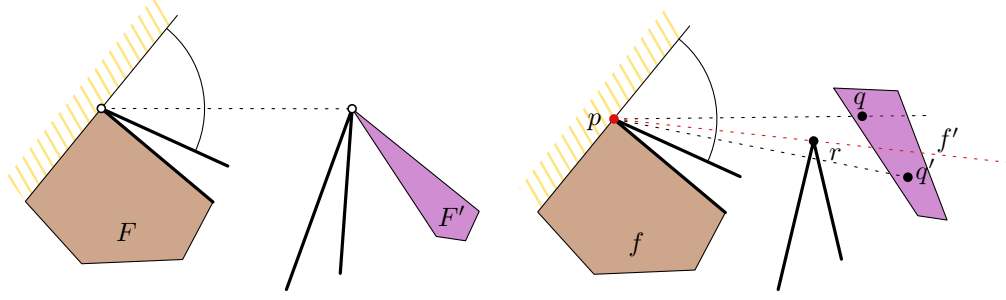


Figure 5: Left: It is not enough for one point of f , seeing one point of f' . We need the stronger assumption that an interior point is seen. Right: If the interior point is seen by the reflex vertex of f , then this reflex vertex sees f' entirely.

We handle first the special case that $a = p$ and no other point of f sees any point in the interior of f' .

Claim 1. *In this case, $a = p$ must be a reflex vertex of P .*

Proof of Claim 1. Consider the chord $\ell = \text{chord}(a, b)$. The chord ℓ does not intersect f in another point a' , as this would imply that a' sees b as well. Thus $a = p$ is a vertex of f and let us assume without loss of generality that ℓ is horizontal, and f is below ℓ . There must be a reflex vertex on ℓ as otherwise, we could slide down ℓ and detect a new visibility pair $(a', b') \in f \times \text{int}(f')$. Now, let r be the rightmost reflex vertex on ℓ . This reflex vertex r must be equal to $a = p$ as otherwise, we can rotate ℓ around r and get a new visibility pair, which does not exist by assumption. This finishes the proof the claim. \square

Due to Claim 1, Lemma 7 implies that $\text{vis}_{\gamma+\delta}(p) \supseteq \text{vis}(p) \supseteq f'$.

Now we consider the case that $a \neq p$. In particular, this implies that a is not a reflex vertex of f . Recall that we want to show for every point $q \in \text{int}(f')$ that $q \in \text{vis}_{\gamma+\delta}(p)$. First note that if the shortest path from p to q ($\text{short}(p, q)$) is the line-segment $\text{seg}(p, q) \subseteq \text{vis}(p) \subseteq \text{vis}_{\gamma+\delta}(p) \subseteq P$, then we are done. Thus, we consider the case that $\text{short}(p, q)$ contains at least one reflex vertex r in its interior. We will show the following claim.

Claim 2. *The shortest path $\text{short}(p, q)$ contains at most one reflex vertex, except potentially p itself.*

Proof of Claim 2. We consider two sub cases.

Subcase 1. First, we consider the case that $\text{short}(p, q)$ is not properly intersecting the line $\ell(a, b)$. In the second case, to be handled later, $\text{short}(p, q)$ properly intersects the line $\ell(a, b)$ once. Note that $\text{short}(p, q)$ cannot properly intersect $\ell(a, b)$ more than once. Otherwise, we could shorten the shortest path by using part of $\ell(a, b)$.

Consider the path $pabq$. When we keep locally shortening this path, we converge to the shortest path. This mental experiment shows that the shortest path forms a convex chain, see Figure 6 a).

For every point t on $\text{short}(p, q)$, we can define a tangent $\text{tangent}(t)$. It holds for every point t that $\text{tangent}(t)$ properly intersects f or f' , except at the very beginning, see Figure 6 b). Now, if $\text{short}(p, q)$ contains two (consecutive) reflex vertices r_1, r_2 , then line $\ell(r_1, r_2)$ is a tangent for some t and thus properly intersects either f or f' . By assumption of the lemma, there is no reflex chord

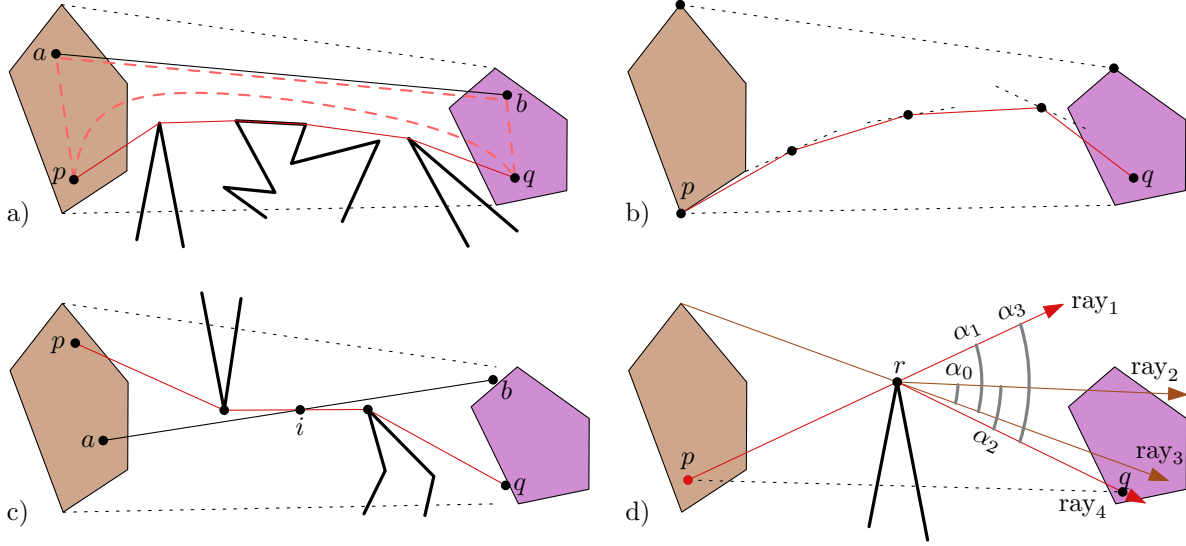


Figure 6: The brown face represents face f and the purple face represents face f' . a) The shortest path from p to q is a convex chain. b) The tangent always intersects either f , or f' . An exception is potentially the tangent through the point p . Recall that q is an inner point. c) In this scenario the shortest path from p to q consists of two convex chains. d) Various rays and angles are illustrated.

that properly intersects either f or f' . The line $\ell(r_1, r_2)$ defines a reflex chord naturally. This finishes the proof of this subcase.

Subcase 2. Now, we consider the second case. That is the shortest path $\text{short}(p, q)$ properly intersects $\ell(a, b)$ in the unique point i . Note that we can now decompose $\text{short}(p, q)$ into $\text{short}(p, i)$ and $\text{short}(i, q)$. By the same argument as in subcase 1, we conclude that $\text{short}(p, i)$ and $\text{short}(i, q)$ are convex chains. We define the path α as the concatenation of $\text{short}(p, i)$ with $\text{seg}(i, b)$. In the same way we define β as the concatenation of $\text{seg}(a, i)$ and $\text{short}(i, q)$. At first note that α and β are fully contained in P and are convex chains. Again, by the same argument as in subcase 1, it holds that every tangent to α and β are properly intersecting either f or f' .

If all reflex vertices of $\text{short}(p, q)$ are on the same side of $\ell(a, b)$, then we can literally repeat the argument from subcase 1. So we assume that there is at least one reflex vertex on either side of $\ell(a, b)$. Let r_1, r_2 be the two consecutive reflex vertices of $\text{short}(p, q)$ such that $\text{seg}(r_1, r_2)$ properly intersects $\ell(a, b)$, see Figure 6 c). Now, note that chord (r_1, r_2) is a reflex chord that properly intersects either f or f' , as $\ell(r_1, r_2)$ is a tangent to both α and β . This is a contradiction to the assumption that neither f nor f' are properly intersected by a reflex chord as stated in the assumption of the lemma. This finishes the proof of Claim 2. \square

Due to Claim 2, we restrict our attention to the case that $\text{short}(p, q)$ contains *exactly* one reflex vertex, denoted by r . By Lemma 7, we know that r sees f' completely, as r sees q , which is an interior point of f' . For an illustration for the remainder of the proof consider Figure 6 d). We define the rays $\text{ray}_1, \text{ray}_2, \text{ray}_3, \text{ray}_4$, which will help us to prove our claim. All rays have apex r . The ray ray_1 has the direction $r - p$. The ray ray_2 describes the boundary of $\text{vis}_\gamma(f)$ w.r.t. f' . The ray ray_3 describes the boundary of $\text{vis}(f)$ w.r.t. f' . The ray ray_4 has the direction $q - r$.

Now, we define the angles $\alpha_0, \alpha_1, \alpha_2, \alpha_3$ as follows. The angle α_0 is the angle between ray_2 and

ray₃. By definition of diminished visibility regions $\alpha_0 = \gamma$. The angle α_1 is the angle between ray₁ and ray₃. It holds that $\alpha_1 \leq \delta/2$, as $\text{power}(f) \leq \delta/2$. The angle α_2 is the angle between ray₂ and ray₄. It holds that $\alpha_2 \leq \delta/2$, as $\text{power}(f') \leq \delta/2$. The angle α_3 is the angle between ray₁ and ray₄. A simple calculation yields $\alpha_3 = \alpha_1 + \alpha_2 - \alpha_0 \leq \delta - \gamma$. This implies that $q \in \text{vis}_{\gamma+\delta}(p)$ and finishes the proof of the lemma. \square

3 One-Shot vision-stable Algorithm

In this section, we will describe an algorithm to solve the art gallery problem.

Theorem 2 (One-Shot vision-stable Algorithm). *Let P be an n vertex polygon, with vision-stability δ and r reflex vertices. We assume that δ is given as part of the input. Then the one-shot algorithm has a preprocessing time of $O(\frac{r^8}{\delta^4} \log n)$ on a real RAM and additionally solves exactly one integer program. The algorithm either returns the optimal solution or it reports that the vision-stability is smaller than δ .*

We call the algorithm from the previous theorem the *one-shot vision-stable* algorithm. Note that this algorithm also verifies that the result it produces is indeed an optimal solution. We call an algorithm with this property *reliable*. For that it does not require the polygon to be vision-stable. This is important as we do not know how to test vision-stability of a polygon. In case that the algorithm does not return the optimal solution the underlying polygon had vision-stability larger than δ . In that case, we can simply half δ and repeat the algorithm. In this way, we can find the optimal solution in the same polynomial running time solving additional $O(\log 1/\delta)$ integer programs in the worst case.

We note that the integer program has size only dependent on r and δ , independent of the input size n . Thus for fixed δ , it holds that the one-shot algorithm is fixed parameter tractable in the parameter r , the number of reflex vertices.

Corollary 10. *The one-shot algorithm is FPT with respect to the number of reflex vertices. This assumes that the input polygons have vision-stability at least some fixed value δ .*

The one-shot algorithm is not actually practical. However, we will describe a second algorithm later, with similar theoretical performance guarantees, which we prove to be able to solve large instances of the art gallery problem practically. Furthermore, we want to point out that while solving an IP may take an exponential amount of time in theory, in our practical experiments it played a minor role for the total running time (see Section 6). This corresponds to experiences that other groups of authors report as well [19].

Note that this algorithm can be implemented in practice and, in contrast to all other implementations that currently exist, the algorithm is guaranteed to find the optimal solution, if the condition of the theorem is met.

Description of the one-shot vision-stable algorithm. As a first step, we construct an arrangement \mathcal{A} . We shoot rays from every reflex vertex and include all those rays to \mathcal{A} . The angle between any two consecutive rays is at most $\delta/2$. We also add all reflex chords to \mathcal{A} . At last, we subdivide all faces that are incident to more than one reflex vertex. Note that we add at most $O(r^2/\delta)$ segments. This finishes the description of \mathcal{A} , see Figure 7. All faces of \mathcal{A} have a power

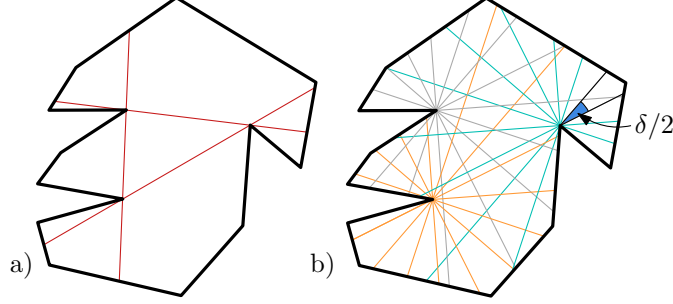


Figure 7: a) We include all chords of all pairwise visible reflex vertices. b) We shot rays from every reflex vertex. The angle between two consecutive rays is at most $\delta/2$. The two sets of segments define together the arrangement \mathcal{A} .

of at most $\delta/2$. Note that \mathcal{A} has $O((r^2/\delta)^2) = O(r^4/\delta^2)$ vertices, edges and faces. This does not account for the convex vertices of P .

We define the candidate set C as the set of all vertices ($\text{vertex}(C)$) that are not convex vertices of P and all faces ($\text{face}(C)$) of \mathcal{A} . We define the witness set W consists of a set of vertices ($\text{vertex}(W)$) and a set of faces ($\text{face}(W)$). For every face of \mathcal{A} , pick an interior point to define the *vertex-witnesses* $\text{vertex}(W)$. The *face-witnesses* are composed of all faces of \mathcal{A} . We call candidates $c \in \text{face}(C)$ *face-candidates* and $c \in \text{vertex}(C)$ *vertex-candidates*. Similarly, we distinguish *face-witnesses* and *vertex-witnesses*.

Next, we compute for every candidate-witness pair $(c, w) \in C \times W$ whether the candidate sees the witness completely. There are $O(r^8/\delta^4)$ such pairs in total. Using appropriate data structures, this can be computed in $O(\log n)$ time [25] per pair.

We are now ready to build an integer program. We call this integer program the *one-shot IP*. For every candidate c , we create a variable $\llbracket c \rrbracket$. For every face-witness w , we create a variable $\llbracket w \rrbracket$. We denote variables with multi-character symbols. As optimization function, we sum all the variables. However, the face-candidates receive a higher weight and the face-witnesses receive a lower weight.

$$f = \sum_{c \in \text{vertex}(C)} \llbracket c \rrbracket + (1 + \varepsilon) \sum_{c \in \text{face}(C)} \llbracket c \rrbracket + \varepsilon \sum_{w \in \text{face}(W)} \llbracket w \rrbracket.$$

We try to minimize the function f . Choosing $1/\varepsilon = |C| + |W| + 1$ is sufficiently small. The function f counts primarily the number of guards that we use. The factor $(1 + \varepsilon)$ ensures that vertex-candidates are preferred over face-candidates. The sum over the face-witnesses counts the number of face-witnesses that we do not see by a single guard in the solution.

For every witness w , we denote by $\text{vis}(w)$ the set of candidates that see w completely. We add the constraints

$$\sum_{c \in \text{vis}(w)} \llbracket c \rrbracket \geq 1, \forall w \in \text{vertex}(W).$$

For the face-witnesses we add the constraints

$$\llbracket w \rrbracket + \sum_{c \in \text{vis}(w)} \llbracket c \rrbracket \geq 1, \forall w \in \text{face}(W).$$

Thus, the constraint to see all face-witnesses is relaxed. However, we need to pay in the objective by ε , for every witness face that we do not see. We also need to add constraints that ensure that every variable is in the set $\{0, 1\}$. The algorithm solves the integer program.

The variables that are set to 1, by the integer program give rise to three sets. A set of *vertex-guards* ($\llbracket c \rrbracket = 1, c \in \text{vertex}(C)$), a set of *face-guards* ($\llbracket c \rrbracket = 1, c \in \text{face}(W)$) and a set of *unseen face-witnesses* ($\llbracket w \rrbracket = 1, w \in \text{face}(W)$). If all guards that are found are vertex-guards and all the face-witnesses are seen by those guards the algorithm reports those point-guards. Otherwise, the algorithm reports that it has not found an optimal solution. In particular, this implies, as we will show, that the input polygon did not have vision-stability δ .

Two stage integer program. While the IP that we describe here works theoretically, when we use a very small value of ε solvers may have trouble in practice. Luckily, there is a simple trick to overcome this, by solving the IP in two stages. The *stage 1 IP* is the one-shot IP, with $\varepsilon = 0$. In other words, the integer program is impartial towards face-guards and vertex-guards. Furthermore, it does not require any face-witness to be seen. Let s be the value of stage 1 IP. In the *stage 2 IP*, we add the constraint that the total number of guards should be s . We define a new objective function f that counts all the face-guards and unseen face-witnesses. We aim to minimize the objective function.

Alternatively, we can also multiply the objective function with $1/\varepsilon$. This seems to work in many situations just as well.

Correctness First note that by the description that we gave the algorithm runs indeed in $O(\frac{r^8}{\delta^4} \log n)$ time and solves exactly one integer program as claimed.

We will first show that the result of the one-shot algorithm is *reliable*. That is, whether the underlying polygon is vision-stable or not, we can trust that the algorithm returns the correct result. Thereafter, we will show that the algorithm will indeed report the optimal guarding for vision-stable polygons.

We show that if all guards G found by the integer program are point-guards and all face-witnesses are seen, then the algorithm indeed returned the optimal solution. Here, we are not assuming that P is vision-stable. As G guards the entire polygon it holds that $|G| \geq \text{opt}$. Let us now consider a set F of point-guards of optimal size. For every $p \in F$, we denote by $\text{face}(p)$ the face of \mathcal{A} that contains p . For some set S of points, we denote by $\text{face}(S) = \{\text{face}(p) : p \in S\}$. Note that $\text{face}(F)$ sees all vertex-witnesses. It may be that there is one or several face-witnesses w that require several faces of $\text{face}(F)$ to be completely guarded. Such a face-witness w , would be counted as unseen face-witness. Still the one-shot IP could use exactly those face-guards $\text{face}(F)$. As the one-shot IP computed a set of point guards G , it implies $|G| < \text{opt} + 1$. Note that $\varepsilon(|G| + |W|) < 1$, by definition of ε . Thus, if the one-shot IP returns a solution using point-guards only and all face-witnesses are seen, we have $|G| = \text{opt}$. This shows that the algorithm is reliable.

Now, we show that if P has vision-stability δ then the one-shot algorithm will return the optimal solution. Let us denote by $s \in \mathbb{Q}$ the value of the one-shot IP.

First, we will show that $s \leq \text{opt}$. As we know that $\text{opt} = \text{opt}(P, -\delta)$ there exists a finite set G , with $|G| = \text{opt}$ such that G is $(-\delta)$ -guarding P . The set G is not necessarily among the vertex-candidates. Using the definitions above, $\text{representative}(\text{face}(g))$ denotes the representative vertex of the face of \mathcal{A} that g is contained in. Note that $\text{face}(G)$ is also $(-\delta)$ -guarding P . (Recall that the visibility of a face f is defined as $\text{vis}_\gamma(f) = \bigcup_{p \in f} \text{vis}_\gamma(p)$.) Thus in particular for every

face-witness w there exists a face $f \in \text{face}(G)$, which sees an interior point of w . By Lemma 8, it holds that there is a vertex $v \in \text{representative}(\text{face}(G))$, such that $w \subseteq \text{vis}(v)$. We apply the lemma with $\gamma = -\delta$. An interior point of w is visible by G , as G is $(-\delta)$ -guarding P . This implies $s \leq \text{opt}$.

The second step is to show that $s \geq \text{opt}$. Let G be the guards returned by the one-shot IP. We construct a new set of point-guards S of size at most s that is δ -guarding P . As $\text{opt}(P, \delta) = \text{opt}$, it holds that $s \geq \text{opt}$. The guards G contains potentially face-guards and may not guard all face-witnesses. However all the vertex-witnesses are guarded. We define $S = \text{representative}(\text{face}(G))$. In other words, for every guard g , consider the face $g' = \text{face}(g)$ that g is contained in. This is g itself, in case that g is a face. In case that g is contained in several faces, pick an arbitrary one. Then consider the representative of that face g' . The set S is the union of all of those representatives. We claim that S is δ -guarding P . To this end let w be a face-witness. Then there is at least one guard in G that sees at least one *interior* point of w , as G sees all vertex-witnesses. (Recall that every face-witness contains one vertex-witnesses by definition.) By Lemma 8, it holds that there is a vertex $v \in S$, such that $w \subseteq \text{vis}_\delta(v)$. (Here, we apply the lemma with $\gamma = 0$.) Thus $\text{representative}(\text{face}(G))$ is δ -guarding P . Thus $s \geq \text{opt}(P, \delta) = \text{opt}$ implies that $s \geq \text{opt}$.

This finishes the proof of Theorem 2. \square

4 Iterative vision-stable Algorithm

The practical bottleneck of the one-shot algorithm is not solving the integer program, but the polynomial time preprocessing step. Our iterative algorithm has several *ideas*, which give huge improvements in practice, while maintaining the theoretical performance guarantees.

The first idea is to maintain a coarse arrangement \mathcal{A} and only refine \mathcal{A} where needed in an iterative fashion. Thus the name iterative algorithm. The refinement is by splitting appropriate faces. In order to identify faces to be split, we will need to modify the integer program. We will modify the integer program such that we will either find a face to be split, find the optimal solution, or conclude that the polygon has not vision-stability δ . In the last case, we can continue with $\delta/2$ as vision-stability. Splitting faces only where needed gives a huge speed-up. The next idea is to reduce the witness set. When we think about witnesses, we noticed that we actually do not necessarily need all witnesses for the integer program. We identify a much smaller set of *critical witnesses*. In the integer program formulation, we require only the critical witnesses to be seen. At a later stage, we check if the guards that we compute in this way are actually guarding everything. We are dynamically increasing the size of the critical witness set. The main advantage is that this does not require us to compute all pairs of visibilities, but only between the guards and the arrangement as well as between the critical witnesses and the arrangement. See Figure 12 for an illustration. Using critical witnesses reduced the number of visibilities that we had to compute largely. However, there were still a large number of visibilities that we had to compute although the two entities (vertex/face) where in completely different parts of the polygon. Our last idea is to compute a subdivision of the polygon, which we call the *weak visibility polygon tree*, see Figure 8. It captures locality of the polygon. Using the weak visibility polygon tree, we can prevent a sizeable fraction of the visibility queries to be even asked.

Let us point out that the iterative algorithm maintains the theoretical performs guarantees as it would in the worst-case subdivide \mathcal{A} , until it is as fine as the arrangement from Section 3. However, in practice most faces will be split much fewer times. We will show the following theorem.

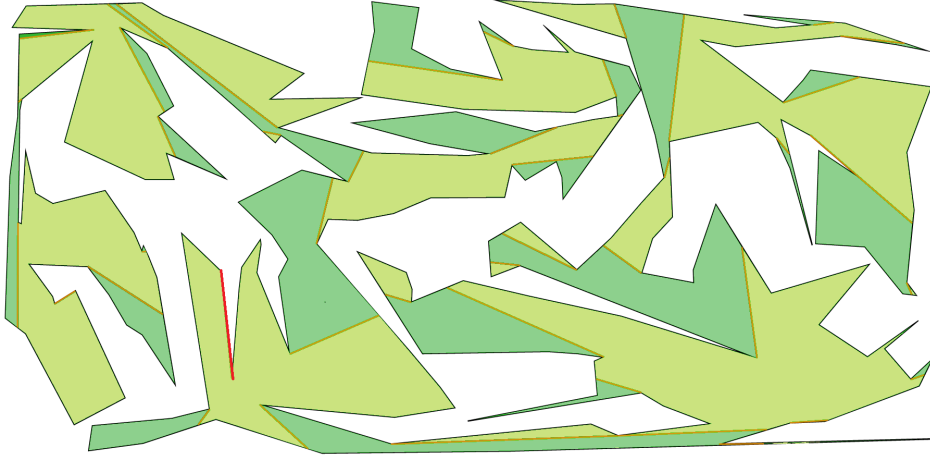


Figure 8: The polygon together with a weak visibility polygon tree. The polygon has 200 vertices, but each node in the weak visibility polygon tree has only about 20 vertices. The red segment indicates the starting edge of the weak visibility polygon tree.

Theorem 4 (Iterative Algorithm). *Let P be an n vertex polygon, with vision-stability δ . Then the iterative algorithm returns the optimal solution to the art gallery problem. It has a running time of $(\frac{n}{\delta})^{O(1)} + T$ per iteration and takes at most $(\frac{n}{\delta})^{O(1)}$ iterations. Here T denotes the time it takes to solve one integer program.*

In the following sections, we describe the iterative algorithm in more detail. Often there are several possible choices. We always describe a “normal protocol”, which is the choice that we consider for Theorem 4. We also define other protocols, as those give huge practical improvements, albeit we cannot prove theoretical performance for them anymore.

4.1 Weak visibility polygon tree

Before, we can start to describe the algorithm in detail, we need to introduce the weak visibility polygon tree. Consider the polygon in Figure 8. Despite the fact that the polygon has many vertices, it seems to have locally low complexity. The idea of the weak visibility tree is to exploit this low local complexity in order to reduce the number of visibility queries to be answered.

To build the weak visibility tree T of P , we start with an arbitrary edge e on the boundary of P . We compute the weak visibility polygon $\text{vis}(e)$ of e , which is the root of T . We use the algorithm by Abrahamsen [1] to compute the weak visibility polygon. For every edge e' of $\text{vis}(e)$, which is not part of the boundary of P , we compute the weak visibility polygon $\text{vis}(e')$ with respect to the polygon $P \setminus \text{vis}(e)$. Those weak visibility polygons are the children of $\text{vis}(e)$. We continue inductively to compute the children of every weak visibility polygon. Note that every node of T is a weak visibility polygon W of some defining chord c . Obviously, c splits P into two polygons Q and Q' , as c is a chord. The weak visibility polygon W is completely contained in either Q or Q' . To be precise, we consider each node of T to be closed and contain its boundary.

Lemma 11 (Saved Visibilities). *Let p, q be in the interior of two different nodes $\text{node}(p), \text{node}(q)$ of T . If $\text{node}(p)$ and $\text{node}(q)$ are neither siblings nor in a parent-child relationship then p, q cannot see each other.*

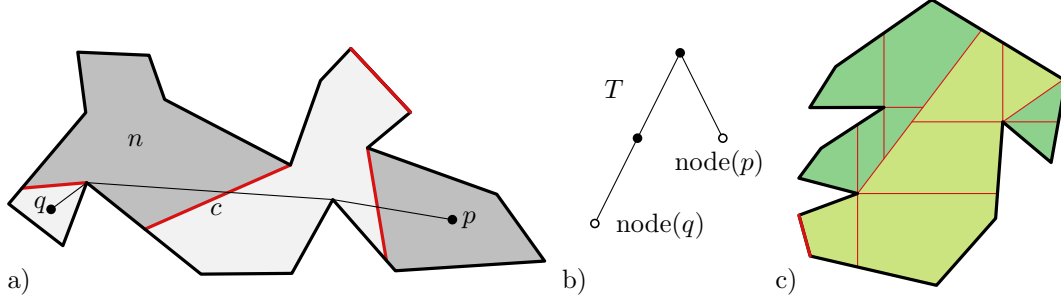


Figure 9: a) & b) The points p and q cannot see each other. Otherwise q , would belong to the node $n = \text{vis}(c)$. c) The arrangement \mathcal{A} is initialized by shooting horizontal rays from the reflex vertices.

Proof. For an illustration of this proof consider Figure 9 a) & b). Consider the shortest path $s = \text{short}(p, q)$ from p to q . We will show that s is not a line-segment and thus conclude that p and q cannot see each other. Note that s will traverse several nodes of T . In particular, it will cross a defining chord c and its corresponding node $n = \text{vis}(c)$. Without loss of generality q is an ancestor of n . Now if s would be a line-segment, then q would be in $n = \text{vis}(c)$. But this is impossible as q is in the interior of $\text{node}(q)$, as stated in the assumption of the lemma. \square

Thus, whenever, we want to compute the set $\text{vis}(p)$, we only need to consider the parent children and siblings of $\text{node}(p)$. This is true whether p is a face or a point. We build a shortest path map for every weak visibility polygon [25]. Those, we will use later in order to answer face visibility queries, see Guibas et al. [25] for details on the shortest path map and how to use it for visibility queries between edges and faces.

4.2 Initialization.

In the initialization phase, we are constructing an arrangement \mathcal{A} , which we will refine in subsequent steps. At first, we add all defining chords c of the weak visibility polygon tree to \mathcal{A} . Furthermore, we shot horizontal and vertical rays from each reflex vertex. We stop the ray as soon as it hits the boundary of the polygon or another edge of \mathcal{A} . See Figure 9 c). We shoot the rays in arbitrary order. There are $O(r)$ defining chords, as each chord, other than the first one, is incident to at least one reflex vertex and no two chords are incident to the same reflex vertex. Furthermore, we are shooting $O(r)$ orthogonal rays. As, we are not introducing any crossings, we conclude that \mathcal{A} has a complexity of $O(r)$, where r is the number of reflex vertices of the polygon. And all faces of \mathcal{A} are convex.

4.3 Splits.

In this paragraph, we assume that some other part of the algorithm identified some appropriate faces to be split. We choose from four different types of splits, called *square split*, *angular-split*, *(reflex) chord split* and *extension split*, see Figure 10.

Square splits. Square splits divide a face using a horizontal and vertical segment, such that the height and width of the new faces are halved. These type of splits have several advantages. They are really easy to compute. They ensure that each new face is only incident to at most one reflex

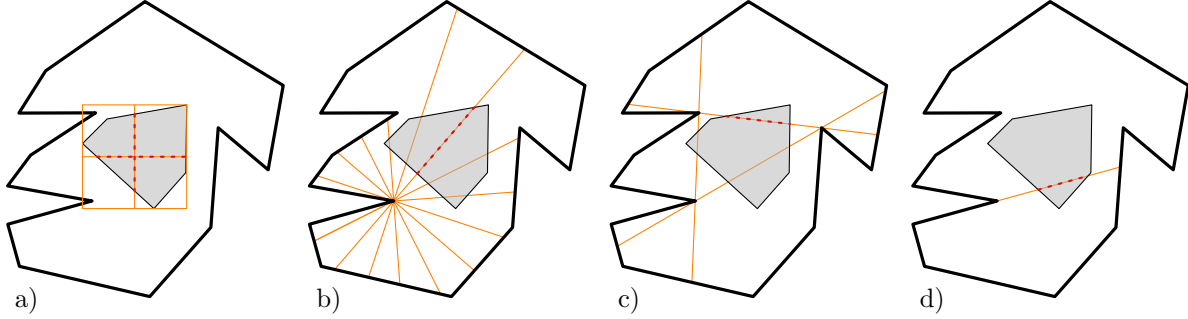


Figure 10: a) square split, b) angular split, c) (reflex) chord split, d) extension split

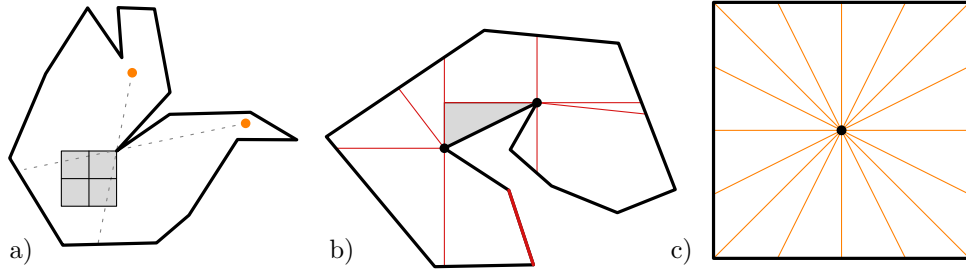


Figure 11: a) The two orange guards, are guarding the entire polygon and the polygon is vision-stable. Still, even after an arbitrary number of square-splits, there remains a face that is neither from the top nor from the right guard completely visible. b) If a face is incident to two reflex vertices, it may guard an entire polygon that otherwise can only be guarded with two guards. Square splits are efficient to ensure that the face is only incident to at most one reflex vertex. c) Directions that we use for angular splits.

vertex. They are reducing efficiently the power of the new faces, if the face was not adjacent to a reflex vertex. Square-splits have to disadvantages. First, it seems non-trivial to upper bound the number of square splits needed to ensure that every face has power at most δ . Secondly, faces incident to reflex vertices do not have their power reduced. See Figure 11 a).

Angular splits. In angular splits, we shoot rays from a reflex vertex, as to reduce the power of the face. One fundamental problem with angular splits is that we are not allowed to use trigonometric functions (sinus, cosinus) in the real RAM model of computation. But those functions are also problematic in practice, as we inherently need to use rounding. As a work around, we consider the rays 2^k as indicated in Figure 11 c). We define the *granularity* of the angular splits as $\lambda = 2^{-k}$. Recall that $\alpha/2 \leq \sin(\alpha) \leq \alpha$ for $\alpha \in [0, \pi/4]$. Thus the angle α between any two rays is bounded by $\pi\lambda \leq \alpha \leq 4\pi\lambda$. We use the granularity to get an estimate of the power of a face. We initialize the granularity with $1/16$ and update it, as we will explain in Section 4.5.

The biggest advantage of using angular splits is that we can easily upper bound how many of them we use in the worst-case. The reason being that angular splits are part of the arrangement from the one-shot algorithm.

Reflex chord splits. Reflex chords are very important for the correctness of Lemma 8. Thus we need to include them. It is not very efficient to compute them though, and we have not encountered a practical situation where missing them would be relevant. Thus, we choose those splits only with low probability. However, we do them, if no other type of split is possible.

Extension splits. Given a reflex vertex r , we can consider the rays with apex r parallel to the two incident edges of r . These rays are commonly called *extensions*. If we want to make an extension split, we check if there is an extension that properly intersects the given face. Those splits can be useful, if an optimal guard happens to lie precisely on an extension.

Unsplittable faces. In order to show performance guarantees, we need to make sure that we are not doing too many splits. For that purpose, we declare faces *unsplittable*, if all of the following conditions are met.

- the face is incident to at most one reflex vertex.
- no reflex chord or extension split is possible.
- the face is not splittable by angular splits of granularity λ . (Here, λ is the current granularity.)

The last item, implies that the power of the face is at most $4\pi\lambda$. In particular, If a face is unsplittable then all conditions of Lemma 8 and Corollary 9 on the faces are met for $\delta \geq 8\pi\lambda$.

Protocol. There are many different ways that we can decide which split to make. Here, we explain two protocols, the normal protocol and the square split protocol. In the *normal protocol*, we do square splits only, if the face is incident to more than one reflex vertex. This will happen only very few times and usually only at the beginning of the algorithm. We choose the angular split with probability 0.8, and the other two remaining split types with equal probability. In case a split is impossible, we will try the other two splits, before deciding that a face is unsplittable. In the *square split Protocol*, we are using always square splits. We know some situations, where square-splits are not good and will make the algorithm run into an infinite loop, see Figure 11. However, for most polygons square splits give a significant performance boost.

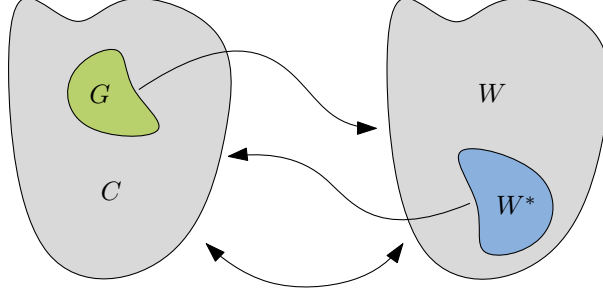


Figure 12: We compute all visibilities between the critical witnesses W^* and the candidates C and then all visibilities between the guards G and the witnesses W .

4.4 Critical Witnesses.

The arrangement \mathcal{A} has many vertices and faces that are not particularly important to be guarded. The idea of the critical witness set is to identify a subset $W^* \subseteq W$ of critical witnesses which are relevant. At the beginning, we initialize the *critical witness* set W^* by randomly picking 10 percent of vertices and faces, for each weak visibility polygon separately. In this way, the critical witness set is roughly equally distributed over the whole polygon. Later, through out the iterations, we add to the critical witnesses set as necessary, by using the guards G given by the integer program. See Section 4.5 for a detailed description of the integer program. We compute all the vertices and faces that G sees. This also gives us the sets of unseen face-witnesses and vertex-witnesses U which were not marked as critical before. We then randomly choose a small constant size subset of vertices and faces from U that we add to W^* . In the practical implementation of the program, the size of this subset of U that we add to W^* depends on the number of cores of the processor of the system that it is run on. Note that if we were to mark all unseen witnesses as critical this would lead to very large numbers of visibility queries, thus defeating the purpose of using the critical witness set. It would also increase the size of all subsequent integer programs that we need to solve. It is important to find a good balance between adding too few critical witnesses and adding too many. Using the number of cores is plausible, because our practical implementation runs the visibility queries in parallel.

Every time we update the critical witness set, we re-run the IP to check if we can find a better solution given the critical witnesses. We keep adding to the critical witness set as long as there are unseen witnesses left that are not marked as critical. We then check if we need to update the new critical witness set again using this new-found guard set. We keep doing these *critical cycles*, until we find a guard set that can see the entire polygon. Only then we split the faces and continue with the next iteration.

A face can only be removed from the critical witness set, if it is split. For every critical witness face, we also add a critical vertex to the interior of that face. Critical witness vertices are only removed from the critical witness set, if they are interior to a face that is removed.

To summarize, we do not need to compute all the visibilities between all the candidates and all the witnesses. Instead, we compute all visibilities between the critical witnesses W^* and candidates C and then all visibilities between the guards G and the witnesses W . As there are much fewer guards than candidates and also much fewer critical witnesses W^* than witnesses overall, this saves a lot of running time in practice.

Protocol. Although the use of critical witnesses gives a big improvement in practice, we cannot show theoretical performance guarantees using critical witnesses. For later reference, we say that we use the *critical witness* protocol in case that we use critical witnesses. Otherwise, we do not use critical witnesses. We also define the *delayed critical witness protocol*. In this protocol, we use critical witnesses and we add all faces, which have a power larger than the granularity $\sqrt{\lambda}$. In this way, we balance theoretical and practical performance.

4.5 Building the integer program.

We need to use in total at most two integer programs per iteration. The *normal IP* and the *big IP*. We want one of the following three scenarios to happen.

1. We find an optimal solution and we can confirm that it is optimal.
2. We find at least one face that we can split and thus make progress.
3. We find that our current granularity λ is too high and we can update the granularity.

Recall that the granularity is an estimate for the vision-stability. In case that we use critical witnesses, we are also content, to find unseen witnesses that we can add to the critical witness set.

Normal IP. The normal IP is literally the same as the one-shot IP. In case the algorithm that we use critical witnesses the normal IP only adds constraints and variables for critical witnesses.

Big IP. Before, we decrease the granularity, we want to make sure that we have not missed a face that we may want to split. We construct the big IP with the purpose of finding a solution involving at least one splittable face. Let us denote by $s \in \mathbb{Z}$ the value of the normal IP rounded down. That is the number of used guards. Given a set S of faces and vertices, we denote the subset of splittable faces by $\text{splittable}(S)$. We define the objective function as

$$f = \sum_{x \in \text{splittable}(W \cup C)} \llbracket x \rrbracket.$$

We aim to maximize the number of splittable faces that are used. They appear either as guards or unseen witness faces. We add several constraints. Every variable is either 0 or 1. We require that the total number of candidates equals s .

$$\sum_{c \in C} \llbracket c \rrbracket = s$$

We also require all vertex-witnesses to be seen. This leads to the following constraint, for every $w \in \text{vertex}(W)$.

$$\sum_{c \in \text{vis}(w)} \llbracket c \rrbracket \geq 1$$

In this context, $\text{vis}(w) \subseteq C$ denotes the set of candidates that see w completely. As we want to identify exactly those witness faces, that we can split, we add the following constraint, for every splittable witness-face $w \in \text{splittable}(W)$.

$$1 - \left(\varepsilon \sum_{c \in \text{vis}(w)} \llbracket c \rrbracket \right) \geq \llbracket w \rrbracket$$

This constraint ensures that

$$\sum_{c \in \text{vis}(w)} \llbracket c \rrbracket \geq 1 \quad \Rightarrow \quad \llbracket w \rrbracket = 0$$

In other words, if there is a guard that sees w , then the corresponding variable $\llbracket w \rrbracket$ must be set to 0.

The solution to the normal IP and to the big IP yield naturally a set of guards ($G = \{c \in C : \llbracket c \rrbracket = 1\}$) and a set of unseen witnesses ($U = \{w \in W : \llbracket w \rrbracket = 1\}$). Reversely, if we have given a set of guards and unseen witnesses, this gives a feasible solution to the normal IP and to the big IP.

IP Protocol. Let us first describe the *normal IP protocol*. We will always use the normal IP. Let us denote by G the set of guards returned by the normal IP. (If there are faces or vertices that are not seen by the guards G , we may add some of them to the critical-witness set, see Section 4.4.) If G contains only vertex-guards and we checked that G sees the entire polygon, then the algorithm reports G as the optimal solution. If either G or the unseen witnesses contain at least one splittable face, we split that face and continue with the next iteration. If none of the above happens, we run the big IP. Again, we check for the same set of events. In case that again none of the events above happen, the algorithm updates our estimate granularity λ .

In practice, it seems that using the big IP rather slows down the running time. Although, we may subdivide the “wrong faces” too many times, it seems not to happen ever. Even worse, running the big IP seems to only prevent us from progressing faster. We define the *simple IP protocol* as follows. Only run the normal IP and split all the faces that are selected as unssen face-witnesses or face-guards, according to Section 4.3. Repeat with the new arrangement.

Granularity Update Protocol. We have two protocols for the granularity update. In the *normal granularity update protocol*, we replace λ by $\lambda/2$. In the *accelerated granularity update protocol*, we replace λ by λ^2 . We can still prove theoretical performance guarantees for the accelerated granularity update protocol. Our estimate on the vision-stability is off by a polynomial factor instead of a constant factor, but this is not an issue, when we want to prove polynomial running times. Thus from the theoretical side this looks great. Let us look at the practical side. It is straight-forward to see that with the accelerated granularity protocol, we have to update λ only $\log \log(1/\lambda^*)$ times. Where λ^* is the final granularity when the algorithm terminates. Thus we are also using almost exclusively the simple IP protocol, as we are only using the big IP in case that we cannot find a splittable face. In other words, the accelerated granularity update protocol seems to combine the best of both worlds.

4.6 Correctness

In this paragraph, we prove Theorem 4. To be precise, we use the normal split protocol, the normal IP protocol, the normal granularity update protocol, and no critical witnesses. (Note with small modifications, we can use the accelerated granularity update protocol and the delayed critical witness protocol and still show performance guarantees.)

The proof is divided into three parts. First, we show that the algorithm is reliable. Second, we show that the algorithm makes progress in each step. Third, we will show an upper bound on the total number of iterations.

Reliability. We prove reliability in the same way that we proved it for the one-shot algorithm. For the benefit of the reader, we repeat the argument. We show that if all guards G found by the integer program are point-guards and all face-witnesses are seen, then the algorithm indeed returned the optimal solution. Here, we are not assuming that P is vision-stable. As G guards the entire polygon it holds that $|G| \geq \text{opt}$. Let us now consider a set F of point-guards of optimal size. For every $p \in F$, we denote by $\text{face}(p)$ the face of the arrangement \mathcal{A} that contains p . For some finite set $S \subseteq P$, we denote by $\text{face}(S) = \{\text{face}(p) : p \in S\}$. Note that $\text{face}(F)$ sees all vertex-witnesses. It may be that there is one or several face-witnesses w that require several faces of $\text{face}(F)$ to be completely guarded. Such a face-witness w , would be counted as unseen face-witness. Still the normal IP could use exactly those face-guards $\text{face}(F)$. As the normal IP computed a set of point guards G , it implies $|G| < \text{opt} + 1$. Note that $\varepsilon(|G| + |W|) < 1$, by definition of ε . Thus, if the normal IP returns a solution using point-guards only and all face-witnesses are seen, we have $|G| = \text{opt}$. This shows that the algorithm is reliable.

Progress per iteration. In this paragraph, we will show that the iterative algorithm makes progress in every iteration. To be specific, we will show that after every iteration one of the following events will happen.

1. We find an optimal solution and we can confirm that it is optimal.
2. At least one face is splittable.
3. We find that $\delta < 8\pi\lambda$.

In case 1, we are done, as the algorithm is reliable and the algorithm terminates. In case 2, we split those faces according to the description given in Section 4.3. In the last case, we halve the granularity λ . It remains to show $\delta < 8\pi\lambda$. We show the contraposition.

Claim 3. *We denote by δ the vision-stability of the underlying polygon P . Let $\delta \geq 8\pi\lambda$ and neither the big IP, nor the normal IP return a splittable face. Then the normal IP will return the optimal solution.*

Proof of Claim 3. We denote by s the value of the normal IP. We will show that $s = \text{opt}$. Before go into the details of the proof note that we defined unsplittable faces exactly so that we can apply Lemma 8 and Corollary 9.

The first step is to show that $s \geq \text{opt}$. Let G_0 be the guards returned by the normal IP. Let us denote by $U_0 \subseteq W$ the set of faces that are not seen by G_0 . By assumption of the lemma all faces in U_0 are unsplittable. We construct a new set of point-guards G_1 of size at most s that is δ -guarding P . As $s \geq |G_0| \geq |G_1| \geq \text{opt}(P, \delta) = \text{opt}$, it holds that $s \geq \text{opt}$. The guard set G_0 contains potentially face-guards. Note that all face-guards of G_0 are unsplittable and thus their power is at most $\delta/2$. We define $G_1 = \text{representative}(G_0)$. That is for a vertex $v \in G_0$, we define $\text{representative}(v) = v$. For a face $f \in G_0$ we define $\text{representative}(f)$ as in Section 2. Let us denote by $U_1 \subseteq W$ the set of unsplittable faces that are not δ -guarded by G_1 . As all face-guards of G_0 are unsplittable, we can apply Corollary 9. This implies that $U_1 \subseteq U_0$ and thus contains only unsplittable faces. To this end let $w \in U_1$ be any face-witness. We will show that w is actually δ -guarded by G_1 . By construction there is an interior vertex $v \in \text{int}(w) \cap W$, which is guarded by some guard $g_0 \in G_0$. Let $g_1 = \text{representative}(g_0)$. Then the power of w and g_0 are at most $\delta/2$.

Furthermore, neither w nor g_0 is properly intersected by a reflex chord. Both faces are incident to at most one reflex vertex. Thus, we can apply Lemma 8. This implies that $w \subseteq \text{vis}_\delta(g_1)$.

To summarize, G_1 is finite vertex set, which is δ -guarding P . Thus $s \geq |G_1| \geq \text{opt}(P, \delta) = \text{opt}$.

As a second step, we show that $s \leq \text{opt}$. As we know that $\text{opt} = \text{opt}(P, -\delta)$ there exists a set G_0 of point-guards with $|G_0| = \text{opt}$ such that G_0 is $(-\delta)$ -guarding P . The set G_0 is not necessarily among the vertex-candidates. Note that the set of faces $G_1 = \text{face}(G_0)$ containing G_0 is also $(-\delta)$ -guarding P . (Recall that the visibility of a face f is defined as $\text{vis}_\gamma(f) = \bigcup_{p \in f} \text{vis}_\gamma(p)$.) We denote by $U_1 \subseteq W$ the set of witnesses that are not seen by any guard in G_1 . Note that as G_0 is $(-\delta)$ -guarding P it holds that U_1 contains only face-witnesses. Thus (G_1, U_1) defines a feasible solution to the normal IP and the big IP. This implies that all faces of G_1 and U_1 must be unsplittable. Otherwise the big IP would have identified those splittable faces. Now, let $G_2 = \text{representative}(G_1)$ be the set of representatives of G_1 . We will show that G_2 is guarding P . Let $U_2 \subset W$ be the set of unseen face-witnesses of G_2 . By Corollary 9 it holds that $U_2 \subseteq U_1$. This in turn implies that U_2 contains only unsplittable faces. Let $w \in U_2$. We show that there is a guard in G_2 that actually sees U_2 . By assumption there is an interior vertex $v \in \text{int}(w)$. And there is a guard $g_1 \in G_1$ that sees v . Let $g_2 = \text{representative}(g_1) \in G_2$ be the representative of g_1 . By the above it can be checked that all conditions of Lemma 8 are met. This implies that $w \subseteq \text{vis}(g_2)$. Thus G_2 guards the entire polygon P . In particular $|G_2| \leq \text{opt}$ and G_2 defines a feasible solution for the normal IP. Thus $s \leq \text{opt}$. \square

Total number of iterations The idea is to upper bound the number of iterations with the number of faces in the final arrangement \mathcal{A}^* of the iterative algorithm. By the the previous paragraph, we split at least one face in every step of the algorithm, except if we lower the update granularity. But we will not do this two times in a row.

Every edge in \mathcal{A}^* comes from one of the following sources.

1. It is part of an extension segment, see Figure 10 d).
2. It is an edge that comes from the boundary of a weak visibility polygon.
3. It comes from a square split in order to prevent that a face contains more than one reflex vertex, see Figure 11 b).
4. It comes from an angular split.
5. It comes from a reflex chord split.

By definition there are $O(r)$ segments of type 1, 2 and 3, here r denotes the total number of reflex vertices of P . Let λ^* be the final value of the granularity. Then there are at most r/λ^* segments of type 4. Here we consider the maximal segment starting at the reflex vertex and not just the edge that split the specific face. By the the paragraph above, we know that this implies that the vision-stability δ is at most $8\pi\lambda$. In other words, there are at most $O(\frac{r}{\delta})$ segments of type 4. By definition there are at most $O(r^2)$ reflex chords. As any two segments intersect at most once, we have at most

$$O\left((r + r/\delta + r^2)^2\right) = O(r^4/\delta^2) = \left(\frac{n}{\delta}\right)^{O(1)}$$

vertices. As the arrangement is planar, this also describes the total number of edges and faces asymptotically.

Each iteration solves at most two IPs and takes polynomial time, this finishes the proof of Theorem 4.

5 Chord-Visibility Width

In this section, we define the notion of *chord-visibility width*, and give a justification, why we believe it to be an interesting parameter in practice. Then, we describe a fixed parameter time algorithms for the art gallery problem. Here the parameter is the chord-visibility width. We denote with *vertex-guarding*, a variant of the art gallery problem, where the guards are restricted to lie on the vertices of the input polygon.

We will show the following two theorems.

Theorem 12. *Let P be a simple polygon. Then there is an FPT algorithm for vertex-guarding P with respect to the chord-visibility width.*

Theorem 5 (Chord-Width-FPT). *Let P be a simple vision-stable polygon. Then there is an FPT algorithm for the art gallery problem with respect to the chord-visibility width.*

We want to point out that the theoretical running times of both algorithms make it prohibitive to use those algorithms in practice. Thus both algorithms are a theoretical contribution to the art gallery problem.

5.1 Definition and Justification

Given a chord c of P , we denote by $n(c)$ the number of vertices visible from c . The *chord-visibility width* ($cw(P)$) of a polygon is the maximum $n(c)$ over all possible chords c .

The chord-visibility width is a way of capturing the local complexity of a polygon, with respect to the notion of visibility. Clearly, not all polygons in practice have small chord-visibility width. We like to think about chord-visibility width, as measure on local complexity. It is noteworthy that many synthetic polygons that are created in a random process have much smaller chord-visibility width than they have reflex vertices. On the other hand, polygons P constructed in many hardness reductions have typically $cw(P)$ roughly proportional to the total number of vertices.

5.2 FPT algorithms

For the rest of this section, we fix k to denote the chord-visibility width of P . As a warm-up, we prove Theorem 12. Let T be, for the rest of this section, the weak visibility polygon tree as defined in Section 4.1. We aim to describe a dynamic programming algorithm on the tree T . We note the following lemmas as a preparation.

Lemma 13. *Let u be a node of T , then u has at most $k = cw(P)$ vertices.*

Proof. Let c be the defining chord of u . Every vertex of u is visible from c . The lemma follows from the definition of chord-visibility width. \square

Given a node u of T , it consists geometrically of several edges and vertices. Some of those edges are part the boundary of P . Other edges are in the interior of P . We call those second type of edges *windows* of u .

Lemma 14. *Let u be a node of T , then u has at most $k = cw(P)$ windows. In other words, every node in u has at most k children and thus also at most k siblings.*

Proof. Any window of u contains at least one reflex vertex, which is visible from the defining chord of u . The lemma follows from the definition of chord-visibility width. \square

We are now ready to prove Theorem 12.

Proof of Theorem 12. Let us denote by V the set of n vertices of P and by R the set of reflex vertices of P . First we construct an arrangement \mathcal{A} defined by $\text{chord}(V, R)$ and the boundary of P . Note that $\text{chord}(V, R)$ consists of $O(n^2)$ line-segments. Thus \mathcal{A} consists of at most $O(n^4)$ edges and line-segments. (Note that we could give even better bounds using chord-visibility width, but they are not needed.) Let $\text{face}(\mathcal{A})$ denote the set of faces of \mathcal{A} . Let u be some node of the weak visibility polygon T , as described in Section 4.1. Let $\text{vertex}(u)$ be the set of vertices of P inside u . We create for each node u of T a table denoted by $\text{table}_1(u)$. We have an entry for every set $S \subseteq \text{vertex}(u)$ and we list all the faces $F \subseteq \text{face}(\mathcal{A})$ that are visible from S . Note that by definition of \mathcal{A} , it holds that every face is either completely seen or not at all from a vertex of P . To construct $\text{table}_1(u)$ takes at most $2^k n^{O(1)}$ time and space, by Lemma 13.

As a next step, we create for every node u a second table $\text{table}_2(u)$. Let W be the set of vertices of the node u and all its children. Clearly W has at most $k^2 + k$ vertices, see Lemma 13 and Lemma 14. For every subset $F \subseteq W$, we store the faces of $\text{face}(\mathcal{A})$ it sees and whether it is possible to completely see all the faces in all descendants of u , using F . And if it is possible, then we also compute how many guards are needed at least, including the guards in S . This is trivial for the leaves of T as the leaves have no children. Now consider a node u with at most k children u_1, \dots, u_k . We consider the case that the tables of $\text{table}_2(u_1), \dots, \text{table}_2(u_k)$ are already created. Then we can create the table $\text{table}_2(u)$ in $O(2^{k^3} n^{O(1)})$, as follows. For every set F , check for all the children, using the previous entries of $\text{table}_2(u_i)$, if the subtree below u_i can be completely seen, and if yes, how many vertices are needed. As T has only $O(n)$ nodes, we can create all tables in $2^{k^3} n^{O(1)}$ as well. In particular, this also creates table_2 also for the root of T . We go through all the entries of the root. We check which of them sees all the faces of the root as well. among those entries, we choose one with the minimum number of guards used. \square

Note that by definition in vertex-guarding all the vertices of P for a candidate set that contains the optimal solution. Now as a corollary of Theorem 2 all the vertices of the arrangement \mathcal{A} (as defined in Section 3 form a candidate set, which contains the optimal number of guards for the art gallery problem.) The proof of Theorem 5 follows along the same lines as the proof of Theorem 5. We need the following lemma as preparation.

Lemma 15. *Let δ be the vision-stability of P and u a node of the weak visibility polygon tree of P . Let chord-visibility width of P be k . Then u contains at most $O(k^6/\delta^2)$ vertices of \mathcal{A} .*

Proof. We first count the number of maximal segments of \mathcal{A} that are at least partially inside u . Note that every reflex vertex of P emits at most $1/\delta$ such chords, by the angular ray shooting. Furthermore, every reflex vertex r can see also at most k other reflex vertices. This bounds the segments from $\text{chord}(R, R)$ associated with r by k as well. Furthermore, the number of reflex vertices in u , its parent or one of its children is upper bounded by $(k+2)k$. Thus there are at most $2k^2(k+1/\delta)$ many segments of \mathcal{A} intersecting u . As any two segments intersect at most once, we get that there are at most $O(k^6/\delta^2)$ vertices of \mathcal{A} inside u \square

We note that the bound in the lemma can clearly be improved. However, the algorithm would still be prohibitively slow. We are focusing here on a simpler exposition rather on getting the best theoretical bounds.

We are now ready to prove Theorem 5.

Proof of Theorem 5. The algorithm is almost identical to the algorithm in Theorem 12. The difference is in the candidate set that we use in each node. Instead of size k it has now size $O(k^6/\delta^2)$. Thus each table has size $O(k^7/\delta^2)$. This changes the running time to $2^{O(k^7/\delta^2)}n^{O(1)}$. \square

6 Test Results

We tested the practical implementation of the Iterative Algorithm, described in Section 4, in several ways. The goal of the first experiment, described in the Section 6.1, was to find out the practical running time of the implementation and how it relates to input factors such as size, chord-visibility width and vision-stability. These tests were performed on random, simple input polygons of different sizes up to 500 vertices. The input polygons were obtained from the AGPLIB library [16], a library used for other papers on the art gallery problem as well [19]. We will describe the polygons in more detail in Section 6.1.

A second experiment was conducted to show that the practical implementation gives iteratively improving guard solutions, even for the irrational guard polygon that requires irrational guards, presented in [2].

Section 6.3 shows the CPU time distribution, showing what percentage of CPU-time is spent on doing which tasks.

The experiments were ran on a computer with a 64-bit Windows 10 operating system, a 8-core Intel(R) Core i7-7700HQ CPU at 2800 Mhz and 16 GB of main memory.

The practical implementation heavily makes uses of version 4.13.1 of CGAL [30]. The IP solver used was IBM ILOG CPLEX version 12.10 [10]. This IP solver was also used by de Rezende et al. [19].

6.1 Practical running times and correctness

To find out how the implementation performs in practice, we tested the algorithm on several input polygons. As mentioned previously, the input polygons were taken from the AGPLIB library [16]. We had access to random simple polygons of different size classes. We tested on 30 instances of polygons of sizes 60, 100, 200 and 500 vertices. An example of one of the 200-vertex polygons and its solution is shown in Figure 13.

For these tests, we used two different versions of the iterative algorithm. The first version is the algorithm that has theoretical performance guarantees. The second version is the same algorithm in spirit, but includes several optimizations that make it perform much better in practice. The correctness of the practical implementation was verified using the implementation provided by Tozoni et al [31]. This implementation was also tested on the same input data-set, which makes it possible for us to cross-check our results to see whether we have found a solution of the correct size.

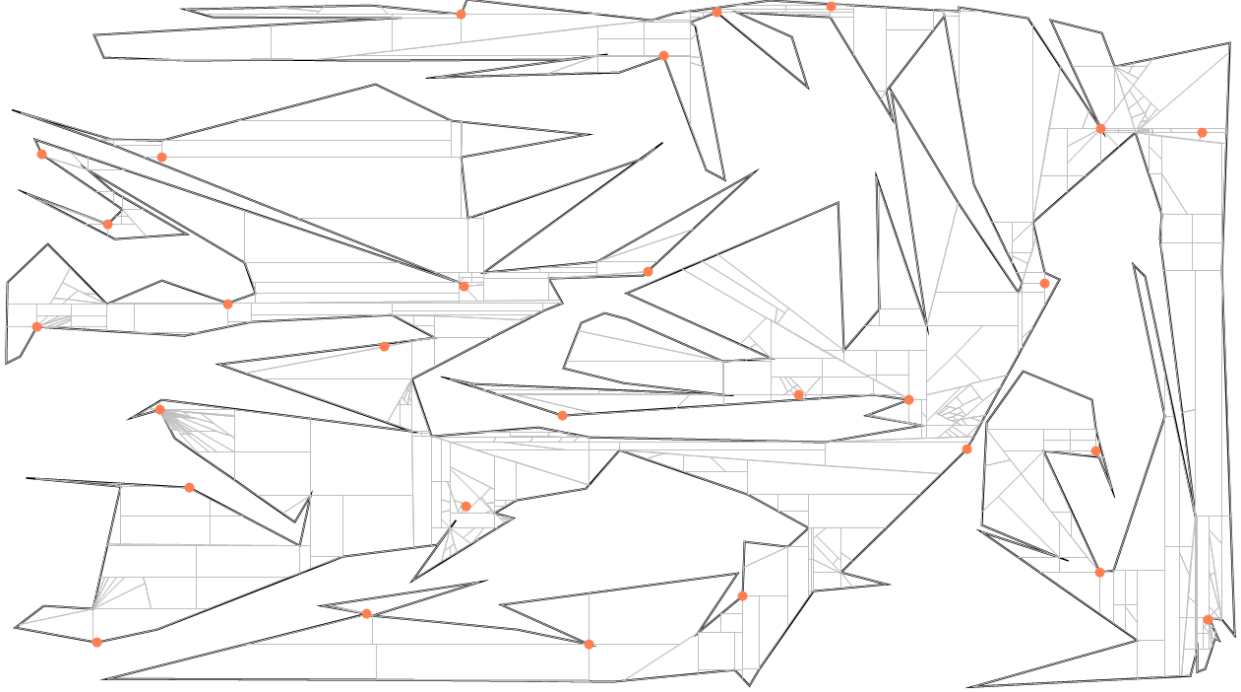


Figure 13: An example of a 200-vertex input polygon and its solution, as found by the iterative Algorithm without safe guards. We have also included the final arrangement at the end of the algorithm.

Iterative Algorithm without Safe Guards. For this version, we opted for the most efficient protocols in practice. This means that we forsake some of the theoretical guarantees that we do not need in practice. See Appendix A for an illustration. For these tests, we used the critical witness protocol. When splitting, we used the normal split protocol. Finally and most importantly, we applied the simple IP protocol, to make sure to make as few unnecessary splits as possible.

Using this variant, we found some reasonable practical results. We were able to find the optimal solutions for all tested instances. The averages and medians for the size classes tested are shown in Table 1. Note that the times we report exclude the pre-processing time of computing the weak visibility decomposition before the first iteration. This table also shows the results by Tozoni et al. [31] pertaining to polygons of these sizes. We acknowledge the fact that the results from Tozoni et al. [31] were improved on by de Rezende et al. [19]. However, we were not able to find the exact running times from this improved version corresponding to these sizes. This table shows that running time of our algorithm is not faster than the algorithm from Tozoni et al. [31], but it is not too far behind. Also, the median running times of this variant of the iterative algorithm is lower than the average running times. We believe this is, amongst other reasons, because the algorithm is sensitive to the vision stability of a polygon. This means that few polygons are very hard to solve and overly influence the average.

Iterative Algorithm with Safe Guards. This is the version of the algorithm from Theorem 4. We did not make use of critical witnesses. For splits, we used the normal split protocol, in which

Sizes	Average time (s)		Median time
	Tozoni et al. (2016)	Ours	
60	0.26	0.67	0.47
100	0.94	2.45	1.6
200	3.77	19.67	6.29
500	35.04	64.52	56.49

Table 1: A comparison of the iterative algorithm without safe guards with the results from Tozoni et al. [31]. Note that the reported times for our algorithm do not include the pre-processing time. Note that the results from Tozoni et al. [31] were found on a system with slightly less powerful hardware: Intel Core i7-2600 at 3.40GHz and 8GB of RAM

we mostly focus on doing splits that guarantee a decrease in the power of the face. Furthermore, we used the normal IP protocol. This means that we use the normal IP at every iteration, and the big IP only if the normal IP did not find a splittable face. We also use the normal granularity update.

After running the tests on polygons of size 60, we found that the algorithm finds the solution in an efficient manner in 25 out of 30 instances. For the other 5 instances, no solution was found after 60 minutes. Looking at the results from the iterative algorithm without safe guards, we found that these 5 polygons seem to have rather low vision stability. To estimate the vision-stability, we use the minimum granularity λ of angular-splits of a face that we split, as a heuristic. The polygons that we were able to solve using this variant had granularity within the $\frac{1}{16}$ - $\frac{1}{128}$ range. From testing the other variant, described in the previous paragraph, we found that the 5 polygons that this algorithm could not solve had granularity values between $\frac{1}{256}$ and $\frac{1}{2048}$.

When we use the big IP, we split until there is no optimal solution with splittable faces. In these instances with low vision stability, this means that we will make many seemingly unnecessary splits. This leads to infeasible running times.

Correlation of Granularity and Running Time As mentioned before, the iterative algorithm is sensitive to the vision-stability of the input polygon. To test this, we saved the smallest granularity λ necessary to find the solution. We did this for the iterative algorithm without safe guards. We then computed the correlation coefficients between the running times and the granularity λ . These coefficients are shown in Table 2. These are fairly strong correlations. Note that the minimum granularity λ might not be the best indication of the vision-stability of a polygon. We actually have no efficient way to compute the vision-stability efficiently. A larger polygon might need a very fine subdivision in one part of the polygon, but can be relatively coarse in other parts.

Besides this, there are several other random factors which influence the running time. For example, the IP chooses an arbitrary optimal solution out of several possible options and the splits we do at each iteration are also chosen randomly. Additionally, the chord-visibility width of the weak visibility polygon tree has some effect on the running time. We believe that these factors account for the fluctuation in the correlations.

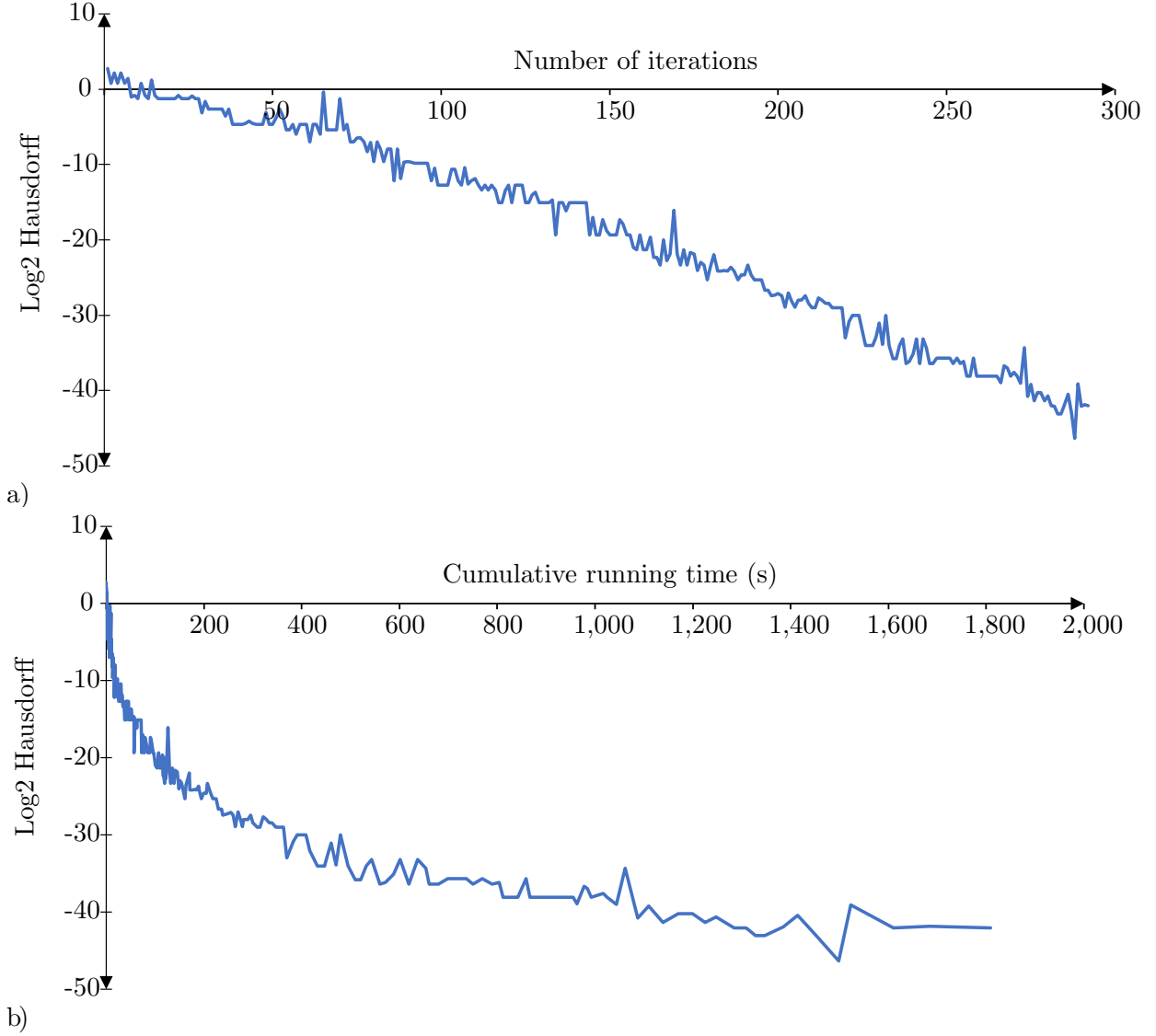


Figure 14: The iterative algorithm based on the notion of vision-stability reports a sequence of solutions. Graph a) shows on the x -axis the iterations from 1 to about 300 and on the y -axis, the \log_2 of the Hausdorff distance to the optimal solution. Graph b) shows on the x -axis the cumulative running time and on the y -axis, the \log_2 of the Hausdorff distance to the optimal solution. All times are in seconds.

Size	60	100	200	500
Correlation	0.73	0.38	0.77	0.45

Table 2: The correlation coefficients between the measured minimum granularity λ and the running time, computed per size.

6.2 Convergence to the optimal solution

In this experiment, we ran the iterative algorithm for 30 minutes, for the irrational-guard-example from [2]. See Appendix A for an illustration of the first 22 iterations. We used the square split protocol, critical witnesses and the simple IP protocol. The results with angular splits and reflex chord splits are similar in spirit, but the convergence is slower. Because we only used square splits, there was no need for the big IP as we did not update the granularity. This polygon is illustrated on the right of Figure 3. Even though the algorithm will not be able to find the optimal solution, we get a set of guards G_i at the end of iteration i . Note that G_i is often a combination of point-guards and face-guards. As we know the optimal solution F , we can compute the Hausdorff distance $d_i = \text{dist}_H(G_i, F)$ at the end of each iteration. See Figure 14 a) for an illustration of the convergence speed per iteration. Interestingly, the distance approaches the optimum very quickly. Additionally, Figure 14 b) shows the Hausdorff distance plotted against the cumulative running time. Here we see that when plotted against the running time, the Hausdorff distance does not decrease as dramatically. This is because the later iterations take more time. That later iterations take more time is plausible. The face splits at every iteration introduces new candidates and witnesses. This means that the IP has to deal with more candidate variables at each iteration and that we have to compute a larger number of visibilities. The appendix includes images produced by the program showing several iterations of the algorithm obtained during this experiment.

6.3 Distribution of CPU usage

This section describes how the workload of the algorithm is distributed on the CPU. To achieve this, we picked three polygons of different sizes and analyzed their CPU usage. The version of the algorithm analyzed here is the best performing variant: the Iterative Algorithm without safe guards. These polygons were chosen because of their running times and how they compare to the average of their size class. The first, smaller polygon performed slower than the average. The second, 500-vertex polygon performed around average while the last 800-vertex polygon was solved faster than average. The 200-vertex polygon used for this analysis is visualized in Figure 13. We performed this analysis using the Visual Studio profiler. [29] Figure 15 shows the results found by the profiler. The CPU usage distribution for other polygons that we tested seemed very similar.

We divided the algorithm into several parts. These different parts are shown in a pie-chart in Figure 15. The first parts, in dark and light blue are both part of the pre-processing step. As described in Section 4.1, to set-up the shortest path map we compute weak visibility polygons and shortest paths. We show in dark blue the time it took to compute the weak visibility polygons of each window while we show in light blue the time spent finding the necessary shortest paths within each of these weak visibility polygons. The part shown in orange are point visibility queries, computing whether a point sees a witness face or witness point. Practically, this is achieved by using the existing CGAL methods, which is based on the triangular expansion method presented in [15]. The chart shows in purple the percentage of the CPU time spent on face visibility queries,

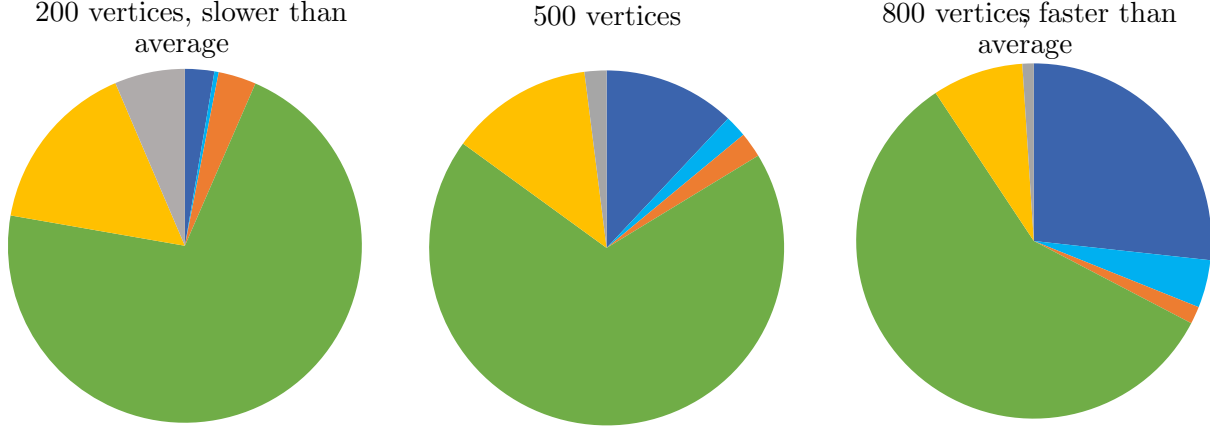


Figure 15: The left chart shows this distribution for a 200-vertex polygon that was slower than average. The middle chart shows the distribution of the workload for a 500-vertex polygon, with an average completion time. Finally, the right chart shows the distribution for a faster-than-average 800 vertex polygon. The dark blue shows the time spent on computing the weak visibility polygons while the light blue is the time it took to compute the shortest paths within each of these weak visibility polygons. The time spent on visibility queries for points and faces are shown in orange and green respectively. The yellow part represents the time to solve the IP. The gray slice represents various smaller tasks.

the question of whether a candidate face guard can see a face or point witness. We also compute these visibilities when checking whether we should add new critical witnesses, as we must make sure that a candidate solution sees the complete polygon. These queries are solved using the shortest path map computed in the pre-processing stage. These face guard visibility queries are done in parallel in our practical implementation. The yellow part shows the CPU time spent on solving the IP using the CPLEX solver. Finally, in gray, other, smaller tasks are combined into one section. These tasks typically consist of updating the intermediate arrangement, splitting faces using our different split techniques and keeping track of the results. We see that, for an average-time polygon such as the 500-vertex example here, most of the time is spent on face-guard visibility and solving the IP. This shows that much running-time improvement could be gained by improving the face-guard visibility routine. When we move on to the slower-than-average polygon, we can see that the workload of most task increase at the expense of the pre-processing part. This makes sense, because the pre-processing time does not depend on the vision-stability and the chord-visibility width like the latter part of the routine does. Finally, looking at the 800-vertex polygon, the inverse happens. The pre-processing time takes a larger chunk of the distribution compared to the other sections of the workload.

The results shown here are for three specific polygons. For the most accurate results, it would have been desirable to repeat this experiment for a large amount of polygons in the testbed. However, running the profiler slows down the algorithm, to the point that running such a large amount of tests would be infeasible. Furthermore, after performing several more of these experiments, we found that these result generalize. From this, we can conclude that the running time of the algorithm is dominated by the face-visibility queries combined with the weak visibility decomposition. Both these subroutines involve computing weak visibilities. We thus believe that most speed-up to

the algorithm could be achieved by implementing more efficient weak visibility routines.

6.4 GitHub code and results

The practical implementation is available at in a GitHub repository <https://github.com/simonheng/AGPracticalWithPerformance>. The folder *results* in the repository contains an excel file which reports the test results discussed in Section 6.1. The code provided in the repository are C++ source and header files, in addition to a Visual Studio solution file. Bear in mind that the code is dependent on CGAL version 4.13.1 [30], IBM ILOG CPLEX version 12.10 [10], the boost library and Libxl version 3.9.0.0 (used to read and write the excel result files). In order to be able to compile and run the project, the above dependencies must be installed.

Acknowledgments We thank Christopher Bouma for letting us use his powerful computer to run our tests. We thank Sofia Rosero Abad for her graphic designs. Furthermore, we would like to thank Marjan van den Akker, Matthew Drescher and Emile Palmieri-Adant for interesting discussions. We thank Pedro de Rezende for helping us to access previous implementations and links to relevant literature. Finally, we thank Édouard Bonnet and Mikkel Abrahamsen for helpful feedback on the presentation.

References

- [1] Mikkel Abrahamsen. Constant-workspace algorithms for visibility problems in the plane. *Master's thesis, University of Copenhagen*, 2013.
- [2] Mikkel Abrahamsen, Anna Adamaszek, and Tillmann Miltzow. Irrational guards are sometimes needed. In *SoCG 2017*, pages 3:1–3:15, 2017. Arxiv 1701.05475.
- [3] Mikkel Abrahamsen, Anna Adamaszek, and Tillmann Miltzow. The art gallery problem is $\exists\mathbb{R}$ -complete. In *STOC 2018*, pages 65–73, 2018. Arxiv 1704.06969.
- [4] Akanksha Agrawal, Kristine V. K. Knudsen, Daniel Lokshtanov, Saket Saurabh, and Meirav Zehavi. The Parameterized Complexity of Guarding Almost Convex Polygons. In *SoCG 2020, LIPIcs*, pages 3:1–3:16, 2020.
- [5] Akanksha Agrawal, Sudeshna Kolay, and Meirav Zehavi. Parameter analysis for guarding terrains. In *SWAT*, 2020.
- [6] Akanksha Agrawal and Meirav Zehavi. Parameterized analysis of art gallery and terrain guarding. In *International Computer Science Symposium in Russia*, pages 16–29. Springer, 2020.
- [7] Yoav Amit, Joseph S.B. Mitchell, and Eli Packer. Locating guards for visibility coverage of polygons. *International Journal of Computational Geometry & Applications*, 20(05):601–630, 2010.
- [8] Pradeesha Ashok and Meghana Reddy. Efficient guarding of polygons and terrains. In *International Workshop on Frontiers in Algorithmics*, pages 26–37. Springer, 2019.
- [9] Patrice Belleville. Computing two-covers of simple polygons. Master's thesis, McGill University, 1991.
- [10] Robert Bixby. IBM ILOG CPLEX. <https://www.ibm.com/analytics/cplex-optimizer>.
- [11] Édouard Bonnet and Tillmann Miltzow. An approximation algorithm for the art gallery problem. In *SoCG 2017*, pages 20:1–20:15, 2017. arXiv 1607.05527.
- [12] Édouard Bonnet and Tillmann Miltzow. Parameterized hardness of art gallery problems. *ACM Transactions on Algorithms*, 16(4), 2020.
- [13] Andrea Bottino and Aldo Laurentini. A nearly optimal sensor placement algorithm for boundary coverage. *Pattern Recognition*, 41(11):3343–3355, 2008.
- [14] Andrea Bottino and Aldo Laurentini. A nearly optimal algorithm for covering the interior of an art gallery. *Pattern Recognition*, 44(5):1048–1056, 2011.
- [15] Francisc Bungiu, Michael Hemmer, John Hershberger, Kan Huang, and Alexander Kröller. Efficient computation of visibility polygons. *arXiv 1403.3905*, 2014.
- [16] Marcelo C. Couto, Pedro J. de Rezende, and Cid C. de Souza. Instances for the Art Gallery Problem, 2009. www.ic.unicamp.br/~cid/Problem-instances/Art-Gallery.

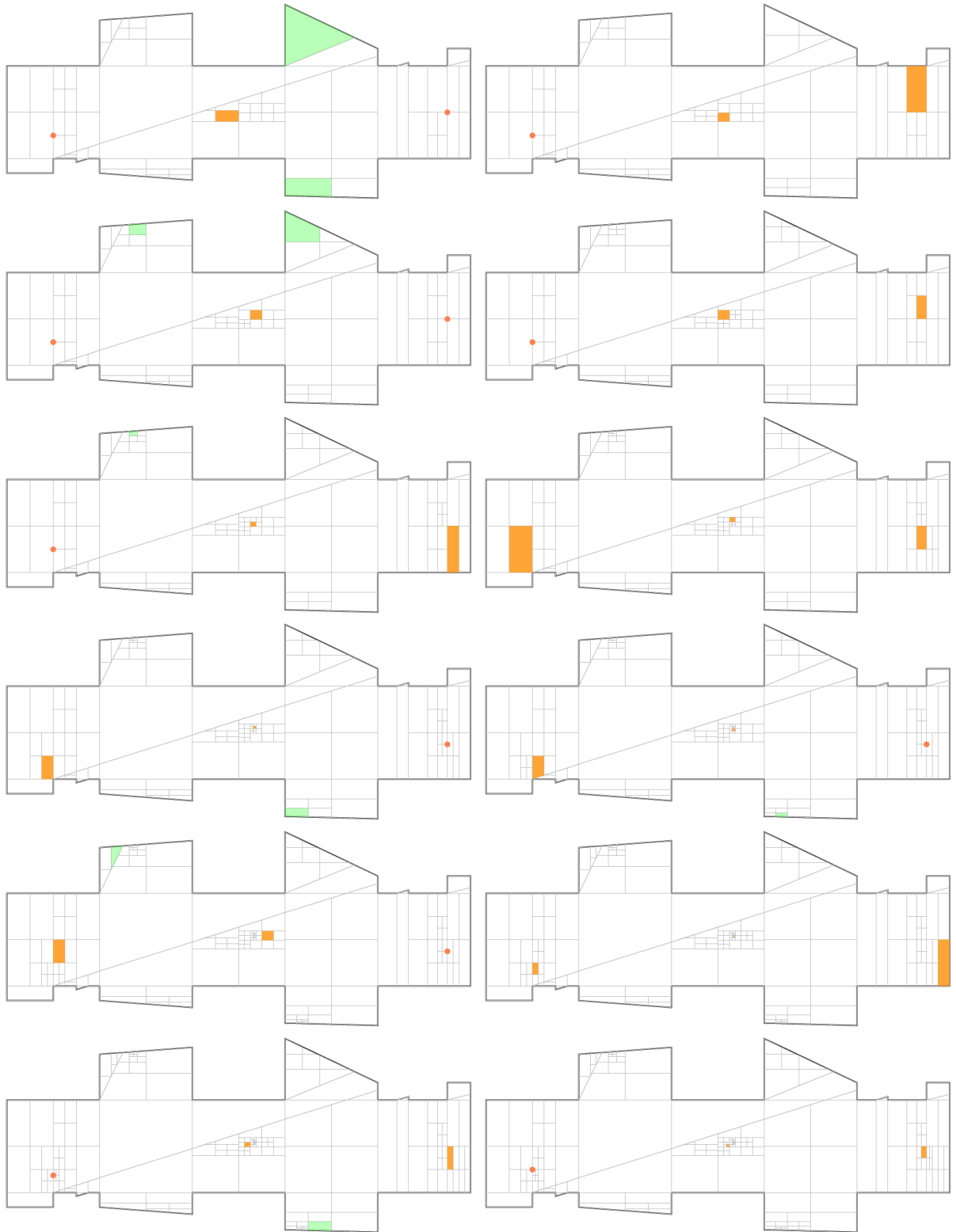
- [17] Marcelo C. Couto, Pedro J. de Rezende, and Cid C. de Souza. An exact algorithm for minimizing vertex guards on art galleries. *International Transactions in Operational Research*, 18(4):425–448, 2011.
- [18] Marcelo C. Couto, Cid C. de Souza, and Pedro J. de Rezende. Experimental evaluation of an exact algorithm for the orthogonal art gallery problem. In *International Workshop on Experimental and Efficient Algorithms*, pages 101–113. Springer, 2008.
- [19] Pedro J. de Rezende, Cid C. de Souza, Stephan Friedrichs, Michael Hemmer, Alexander Kröller, and Davi C. Tozoni. Engineering art galleries. pages 379–417, 2016.
- [20] Michael Gene Dobbins, Andreas Holmsen, and Tillmann Miltzow. Smoothed analysis of the art gallery problem. *arXiv*, 1811.01177, 2018.
- [21] Alon Efrat and Sarel Har-Peled. Guarding galleries and terrains. *Inf. Process. Lett.*, 100(6):238–245, 2006.
- [22] Jeff Erickson, Ivor van der Hoog, and Tillmann Miltzow. Smoothing the gap between NP and $\exists\mathbb{R}$. *accepted to FOCS 2020*. arXiv 1912.02278.
- [23] S. Friedrichs. Integer solutions for the art gallery problem using linear programming. Masterthesis, 2012.
- [24] Panos Giannopoulos. Open problems: guarding problems, 2016.
- [25] Leonidas Guibas, John Hershberger, Daniel Leven, Micha Sharir, and Robert Tarjan. Linear-time algorithms for visibility and shortest path problems inside triangulated simple polygons. *Algorithmica*, 2(1-4):209–233, 1987.
- [26] Farnoosh Khodakarami, Farzad Didehvar, and Ali Mohades. A fixed-parameter algorithm for guarding 1.5 d terrains. *Theoretical Computer Science*, 595:130–142, 2015.
- [27] Farnoosh Khodakarami, Farzad Didehvar, and Ali Mohades. 1.5 d terrain guarding problem parameterized by guard range. *Theoretical Computer Science*, 661:65–69, 2017.
- [28] Alexander Kröller, Tobias Baumgartner, Sándor P. Fekete, and Christiane Schmidt. Exact solutions and bounds for general art gallery problems. *Journal of Experimental Algorithmics (JEA)*, 17:2–3, 2012.
- [29] Microsoft. Visual Studio Profiler. <https://docs.microsoft.com/en-us/visualstudio/profiling/?view=vs-2019>.
- [30] The CGAL Project. *CGAL User and Reference Manual*. CGAL Editorial Board, 4.1.3 edition, 2020.
- [31] Davi C. Tozoni, Pedro J. de Rezende, and Cid C. de Souza. Algorithm 966: A practical iterative algorithm for the art gallery problem using integer linear programming. *ACM Trans. Math. Softw.*, 43(2), August 2016.

A Intermediate Arrangements

Irrational-Guard Polygon.

Below we show the first 22 iterations of the Irrational-Guard polygon. Section 6.2 shows that this iteratively updating set of guards converges to the optimal solution. The orange points and faces represent point- and face-guards in the intermediate solution. The green faces represent faces not fully seen by the current candidate solution. Both orange and green faces are split in the next iteration.





Polygon with 60 vertices.

Here, we show how the Iterative Algorithm without Safe Guards finds a solution in 9 iterations for a polygon with 60 vertices. This is one of the input polygons from Couto et al. [16].

